Nonlinear Dynamics of Avian Influenza Epidemic Models

Final Report

Course name: Mechanical Engineering
Student name: Richard Melville Martin Cheatle

Table of Contents

1. Abstract

Avian influenza is a highly infectious and fatal disease in bird populations that is also able to cause severe disease in humans. Understanding the dynamics of the disease is of great importance in order to control its spread due to the large potential economic and health impacts. This is done by using modelling techniques, such as Kermack-McKendrick SIR equations, to represent the spread using systems of ordinary differential equations (ODEs). This project required a comprehensive literature review of avian influenza in order to understand the characteristics of the disease and how different factors impact the spread. To gain a better understanding of the behaviour of nonlinear systems, the simpler system of Lotka-Volterra equations was modelled using MATLAB and the dynamics studied, before modelling the more complex epidemic and endemic SIR equations. A final model was created using MATLAB that simulated the dynamics of avian influenza in human and poultry populations, with the parameter values fitted to data from previous outbreaks.

2. Introduction

Human diseases are closely linked to epidemics in animal populations. Recent urban and agricultural expansion has increased the amount of contact between animals and humans, through encroachment on animal habitats, domestication of livestock, as well as the keeping of household pets. Due to the close proximity of humans and animals, animal diseases frequently jump across the species barrier and cause human infection. Examples of this include SARS from bats, HIV from monkeys and avian influenza from birds. Around 60% of all human infections and 75% of new emerging human diseases have their origins in animals [20]. Therefore, it is crucial to understand disease dynamics in both animals and humans and to analyse the effectiveness of different ways to control the disease, as it can have great health implications. Models of the dynamics of epidemics were successful in aiding the control of the SARS outbreaks in 2003 and the 2001 UK foot-and-mouth disease outbreak [24].

This project will look at the dynamics of avian influenza virus in both humans and birds. Avian influenza type A virus is a zoonotic infection, meaning that it has previously passed from animal to human. Human infections have been sporadic, and although it is not currently able to cause sustained human-to-human transmission, it has the potential to mutate in future and adapt to mammals. This is of great concern as human infections of avian influenza can result in severe illness and death, and has potential to have devastating health impacts. The biggest influenza pandemic occurred in 1918, and resulted in the death of 20 million people [1]. Occurrence of outbreaks in poultry have increased with the rise of intensive industrial farming due to the high density of animals. This is a result of a high demand for poultry products, with around 20% of protein now coming from poultry in developing countries [7]. Outbreaks can have huge economic impacts, with the 1983-84 outbreak in the USA leading to the destruction of 17 million birds, costing US $56 million [24].

This project will require a comprehensive literature review of avian influenza in order to understand the characteristics of the disease and how different factors impact the spread of the disease. It will also look at epidemic modelling techniques, such as Kermack-McKendrick equations, and how they can be applied to avian influenza to analyse the dynamics of the disease.

3. Literature Review

What is Avian Influenza?

Avian influenza type A viruses are a major concern due to their huge potential economic and health impacts. If avian influenza gains the capability of transmitting from human-to-human then it could cause a pandemic that would potentially cost millions of human lives and cause huge monetary losses. These viruses occur naturally in wild aquatic birds all over the world, but can also affect other birds and animal species. The infection is usually subclinical and hard to observe in wild aquatic birds, but can be highly contagious and fatal when passed onto other species [4][5]. The virus is shed by infected birds through their saliva, nasal secretions, and faeces [6][7]. Avian influenza is categorised as either Low Pathogenicity Avian Influenza (LPAI) or Highly Pathogenic Avian Influenza (HPAI)). LPAI infections may cause no disease or very mild illness, such as a drop in egg production or ruffled feathers. HPAI is a very contagious, multi organ disease which can cause high mortality [4][5].

Domesticated birds, such as turkeys and chickens, can become infected through direct contact with disease carrying birds or contaminated surfaces. LPAI and HPAI viruses can both spread rapidly through flocks, with HPAI viruses capable of wiping out entire flocks within 48 hours [5]. LPAI strains

can potentially evolve into HPAI strains in poultry, especially when the birds are kept close to each other and have genetic homogeneity [5]. During the 1990s, poultry production grew 23% in developed countries, and 76% in developing countries [7]. The number of outbreaks has risen due to the high density of poultry and the regular movement of birds over large distances in commercial farming, making it harder for the virus to be contained. Other significant industries that affect the spread of the virus are village poultry, live bird markets and cock fighting. This is due to the low hygiene, movement of birds and close contact with humans. Other factors that affect the spread include seasonal temperatures, with spikes in cases during the winter months, and wild bird migration. Illegal and legal poultry trades are also thought to contribute to the spread as infection patterns follow transport routes such as roads, country borders and railway systems, such as the trans-Siberian railway [4][8].

In order to control outbreaks, regular surveillance and vaccination of the poultry is carried out. If an outbreak occurs, flocks that have been exposed are culled. In the 2003 and 2004 outbreaks in Vietnam, 44 million birds were culled, approximately 17.5% of the total poultry population [9]. Although culling prevents the immediate spread of HPAI, it impedes the development of host immunity, which is necessary for long term control and has massive economic impacts [10].

Avian influenza has many subtypes, but only five have been found in humans, with the most prevalent being H5N1 and H7N9. Most human cases are the due to the handling of infected birds during slaughter or plucking, as well as contact with infected fluids and contaminated surfaces. Therefore, there is a high level of risk on farms where there is low hygiene conditions [11]. There is no evidence that people can be infected by consuming properly cooked poultry or egg products, but it is possible to be infected by consuming undercooked poultry, raw blood or contaminated water [12]. Human-to-human transmissions are currently very rare, however the virus has the potential to mutate and result in sustained transmission between humans. This may be sped up by human and avian influenzas mixing and exchanging genetic material in infected humans or pigs, who are susceptible to both human and avian influenzas as well as swine flu [8]. Cats are also able to catch avian influenza viruses from contact with infected birds. 20% of stray cats near a poultry market in Jakarta were found to have antibodies for H5N1 after an outbreak in 2007, with it being likely that many more died after contracting the virus [13]. Cats being reservoirs for avian influenza is another potential way that the virus can adapt to mammals and cause a pandemic. Pandemics are the result of contagious novel viruses, never seen before in humans, quickly moving through the population due to a lack of immunity.

Past Outbreaks of Avian Influenza

HPAI was first detected in 1878 in poultry flocks in Italy, however it is unlikely this was the first occurrence of the disease. Dispersed outbreaks continued until the 1950s. Between 1959 and 1995 there were 15 HPAI outbreaks, but the poultry losses during these outbreaks were minimal. Outbreaks became more common and serious between 1996 and 2008, with there being at least 11 outbreaks of HPAI, and millions of birds being involved in 4 of these outbreaks. The H5N1 virus has affected over 60 countries [4]. The first known human cases were during the 1997 Hong Kong H5N1 outbreak, where 18 infections lead to 6 deaths and the poultry population decreased by 1.3 million [6]. Between 2003 and 2019, 861 cases of H5N1 have been reported across 17 countries, with 455 cases resulting in death, a mortality rate of 52.8% [14]. However, there may have been cases that were mild, asymptomatic, undiagnosed or not reported to the World Health Organisation (WHO) by the national governments. In 2006, 9 South Korean poultry industry workers were found to have antibodies for H5N1 after 2427 workers were tested, but did not experience any illness [15]. H5N1 cases have been

more lethal in teenagers and young adults, whilst older patients have had milder symptoms and were more likely to survive [16].

H7N9 was first reported to infect humans in China in 2013. Many of the human cases were linked to live bird markets [17]. H7N9 is the first LPAI that has been known to cause severe disease in humans. As it does not kill poultry, it is hard to detect [18]. From 2013 to 2018, there were 1566 cases of human infection which resulted in 569 deaths, a mortality rate of 36.3% [19]. H7N9 has an estimated median incubation period of 4 days, with a range of 3-7 days [18].

Previous Models of Pandemics

Several mathematical models have been made of avian influenza epidemics in order to simulate the transmission of the disease. Mishra and Sinha [1] developed a mathematical model that considered both the human and bird population. The human population was broken down into the 6 classes of susceptible, exposed, infected, in quarantine, recovered and vaccinated, with each class being represented by an ODE. The bird population was represented by the 3 classes of susceptible, exposed and infected. The equations took into account parameters such as total population, natural birth rate, infectivity, rate of transmission, natural death rate and death rate due to avian influenza. This information was then used to create equations for the human and bird population reproduction numbers. The system was proven to be both locally and globally asymptomatically stable, and converge to the disease free equilibrium point when the reproduction numbers are less than 1. Different values for the different parameters were then used to create simulations and the importance of quarantining and vaccination were assessed. This model could be extended to include recovered and vaccination classes in the bird population.

Zhang, Li, Jin and Zhu [2] developed a mathematical model which took into account the effect of poultry vaccination on the spread of H7N9 after a vaccine program was implemented in China in 2017, as well as the effect of seasonal temperature on the survival of the virus on contaminated surfaces. This model considered the spread through human, bird and poultry populations, as well as the concentration of the virus in the environment. It was assumed that the only way humans could become infected is through environment-human and poultry-human. The human population was broken down into the four classes of ordinary recovered, infected, susceptible and high-risk susceptible. The bird population was broken down into susceptible and infective, and the poultry population was broken down into susceptible, vaccinated and infective classes. Each class was represented by an ODE, as well as another ODE representing the change in concentration of the virus in the environment. Each ODE was made up of parameters such as transmission and birth rates, as well as natural death rates and the H7N9 infection mortality rate. A relationship between temperature and the environmental transmission rates was also obtained and an equation for the basic reproduction number was found. If the reproduction number was below 1, the system was globally asymptomatically stable, and would converge towards the disease free equilibrium. If it was above 1, the disease will continue to spread. The model also looked at the effect of closing live poultry markets and farms as well as frequency of disinfection of the environment. Numerical simulations showed that infection rates are higher in colder temperatures, and that vaccinating poultry significantly reduces the number of human infections.

Liu, Pang, Rhuan and Zhang [3] created a model that studied the transmission dynamics of avian influenza from birds to humans, taking into account the saturation effect within the bird population and the psychological effect of the outbreak and behavioural changes of the general public. The model assumed no human-to-human transmission and birds were the main source of infection. The bird population was separated into the two classes of infective and susceptible, and the human population

was split into the classes removed, infective and susceptible. The model assumed a saturation of the incidence rate due to the crowding of diseased birds or the control measures that would be taken by farmers. It also takes into account how as the number of infected humans goes up, it is likely humans will avoid contact with the birds, for example by not attending wet markets. Each class was represented by an ODE made up of different parameters, such as recovery rate and rate of transmission. Sensitivity analysis of the basic reproduction number was used to give suggested control measures, such as shortening the birds lifetime, reducing bird birth rates and reducing contact between infected and susceptible birds. The saturation effect in the bird population, the transmission rate and the psychological effect in the human population did not affect the stability of the equilibria, but can have an impact on the number of humans infected. This model could be extended to include wild bird populations to improve its accuracy of simulating real world epidemics.

4. Aims, Objectives and Scope of the Project

Aim

The aim of this project is to understand the behaviour of avian influenza, based on previous outbreaks, and construct an avian influenza model. MATLAB will be used to study the dynamics of a model based on a system of first order differential equations and complex nonlinear phenomena.

Objectives

To Undertake a Literature Review of Avian Influenza

A literature review of avian influenza and epidemic modelling techniques will need to be carried out for this project. Understanding avian influenza is necessary as it is important to know the characteristics of the disease, how it behaves as well as how different factors influence the spread of the disease. It is also important to understand how modelling techniques and systems of first order ordinary differential equations are used to simulate and analyse the dynamics of epidemics. For this project an understanding of the mathematics behind techniques such as Lotka-Volterra and SIR equations will be needed, as well as an understanding of how they are applied. Research will be carried out to see how these techniques have been used in the context of avian influenza models. A majority of this literature review will be carried out by looking at scientific journals and papers, as well as internet articles.

To Create Models using MATLAB and Perform Simulations

Once there is an understanding of avian influenza and epidemic modelling, MATLAB will be used to create models and perform simulations. Initially, the simpler systems of Lotka-Volterra and SIR equations will be modelled in order to gain an understanding of how the equations work and behave. A more complicated SIRSI model will then be developed, with parameter values based on data from previous avian influenza epidemics. Results from simulations will then be discussed and analysed. Time been assigned to improving proficiency on the MATLAB software, as these skills will be vital for the simulation of the models. Information for this will be from previous years university material as well as information from the internet.

Scope

The scope of this project includes developing a model that represents the behaviour of avian influenza. This will be done by first constructing simpler models to gain an understanding of nonlinear dynamics

and the MATLAB software, before moving onto a more complicated SIRSI system. This project will be limited by the time available due to other academic responsibilities and the length of the university year. The final model will also be limited to a simpler system due to the lack of previous experience in the subject area.

5. Deliverables

This project has three main deliverables: the progression report, the interim report and the final report. As part of these reports it will be necessary to undertake a literature review and use MATLAB to produce several models. These models will include a Lotka-Volterra model, an epidemic SIR model, an endemic SIR model, a model that fits an SIR curve to input data, an SIRSI model that assigns parameter values based on data from previous avian influenza outbreaks and an SIRSI model that represents the behaviour of avian influenza based on previous outbreaks. To support the reports there will be an oral presentation as well as a logbook that tracks the projects progression.

6. Project Approach and Theory

MATLAB

For this project, different systems of ODEs will be solved using MATLAB in order to allow analysis of their solutions. MATLAB ode solvers use the Runge-Kutta method to give an approximation of the solution over a given time interval. Ode45 is the most commonly used solver for nonstiff equations, however ode15s and ode23s are needed when ode45 is slow or fails and it is possible that the system is stiff [29]. Stiff equations are differential equations that can have rapid variation in the solution. In order to be solved reliably, extremely small steps would be required. This can cause solvers to either take a long time or fail completely [30]. Stiff solvers have been designed for stiff equations which do more work each step and are therefore able to take much larger steps and have improved numerical stability. If ode15s is found to be inefficient, ode23s is used [29].

Lotka-Volterra Equations

In order to understand the basic dynamics of nonlinear differential equations, a simple two equation Lotka-Volterra system will be modelled and studied. Lotka-Volterra equations, also referred to as predator-prey equations, are a set of first order nonlinear ODEs used to describe the dynamics of biological systems. They can be used to show how the predator and prey populations change as the two species interact. An example of a pair of equations is shown below:

$$\frac{dx}{dt} = \alpha x - \beta xy, \qquad (1)$$

$$\frac{dy}{dt} = \delta xy - \gamma y, \qquad (2)$$

where x is the number of prey, y is the number of predators, $\frac{dy}{dt}$ and $\frac{dx}{dt}$ are the rates of change of the populations, t is time and α, β, δ and γ are all real, positive parameters describing the relationship between the two animals [20][21].

The model uses several assumptions. These include that the prey population has a consistent source of food, the predator is reliant on the prey as a food supply, the rate of change in population is proportional to the size, the predators have a hunger that is never satisfied, the environment does not change and

there is no genetic mutation. In equation (1), αx is the growth rate of the prey population with no predation, and βxy is the rate of predation, which is proportional to the rate at which the prey and predators meet. For equation (2), δxy is the growth rate of the predator population, and γy is the decline of predator population due to natural death or emigration [20][21].

The Lotka-Volterra model has an extinction equilibrium at:

$$\mathcal{E}_0 = (0,0). \qquad (3)$$

There is also an equilibrium where the populations coexist at:

$$\mathcal{E} = \left(\frac{\gamma}{\delta}, \frac{\alpha}{\beta}\right). \qquad (4)$$

The stability of the systems fixed points can be found using the Jacobian matrix, or community matrix, of the predator prey model:

$$J(x,y) = \begin{bmatrix} \alpha - \beta y & -\beta x \\ \delta y & \delta x - \gamma \end{bmatrix}. \qquad (5)$$

For the extinction fixed point, the Jacobian matrix is:

$$J(0,0) = \begin{bmatrix} \alpha & 0 \\ 0 & -\gamma \end{bmatrix}, \qquad (6)$$

giving eigenvalues of:

$$\lambda_1 = \alpha, \qquad (7) \quad \lambda_2 = -\gamma. \qquad (8)$$

As the parameters are positive, eigenvalues will always have different signs. This means that this fixed point is a saddle point, and hence unstable. Therefore, populations of prey and predator can get close to zero and still recover.

The Jacobian matrix at the second fixed point is:

$$J\left(\frac{\gamma}{\delta}, \frac{\alpha}{\beta}\right) = \begin{bmatrix} 0 & -\frac{\beta\gamma}{\delta} \\ \frac{\alpha\delta}{\beta} & 0 \end{bmatrix}, \qquad (9)$$

giving eigenvalues of:

$$\lambda_1 = i\sqrt{\alpha\gamma}, \qquad (10) \quad \lambda_2 = -i\sqrt{\alpha\gamma}. \qquad (11)$$

The eigenvalues are both imaginary and conjugate to each other, meaning this point is elliptic and the solutions are periodic, oscillating on an ellipse around the fixed point [20][21].

Epidemic SIR Model

Once the Lotka-Volterra equations have been understood, a model for a more complicated SIR system will be created and studied. Kermack-McKendrick SIR models are very similar to Lotka-Volterra equations and are used to analyse the dynamics of the spread of a disease within a population. A first order ODE is used to represent the susceptible population (S), the infectious population (I) and the removed or recovered population (R), meaning those that have died or recovered from the disease. An example set of these ODEs are given below:

$$N(t) = S(t) + I(t) + R(t), \qquad (12)$$

$$S'(t) = -\beta IS, \qquad (13)$$

$$I'(t) = \beta IS - \gamma I, \qquad (14)$$

$$R'(t) = \gamma I, \qquad (15)$$

where S is the susceptible population, I is the infected population, R is the removed population, N is the sum of the three populations, β is the transmission coefficient and γ is the recovery rate. This model assumes infected individuals are always infectious, the total population size remains constant and the recovered population are immune [28].

During an epidemic, some of the susceptible population never have the disease. The maximum possible susceptible population at the end of an epidemic, S_{max}, is given by:

$$S_{max} = \frac{\gamma}{\beta}. \qquad (16)$$

The peak for the infected population is given by:

$$I_{max} = -\frac{\gamma}{\beta} + \frac{\gamma}{\beta}\ln\frac{\gamma}{\beta} + S_0 + I_0 - \frac{\gamma}{\beta}\ln S_0\,, \qquad (17)$$

where S_0 is the initial susceptible population and I_0 is the initial infected population.

The basic reproduction number, $\mathcal{R}_0$, is the number of expected new infections from a single infection in a population where everyone is susceptible. The initial behaviour of the infected population can be obtained by substituting $S(0) = S_0$ and $I(0) = 1$ into equation 14:

$$I'(0) = \beta S_0 - \gamma = \frac{\beta S_0}{\gamma} - 1. \qquad (18)$$

For this set of ODEs, reproduction number is given by:

$$\mathcal{R}_0 = \frac{\beta S_0}{\gamma}. \qquad (19)$$

If $\mathcal{R}_0 < 1$, it is not an epidemic, and the disease free equilibrium will be locally asymptomatically stable, causing the infected population to monotonically approach 0. If $\mathcal{R}_0 > 1$, then there is an epidemic, and will be unstable, causing the infected population to have nonmonotone behaviour and increase to a peak before decreasing to zero [20][23].

Endemic SIR Model

Epidemic models are implemented to recreate the behaviour of short term outbreaks that take place over the course of less than a year. To study outbreaks over longer periods endemic models are used which take into account the populations birth and death rates, also known as the vital dynamics:

$$N(t) = S(t) + I(t) + R(t), \qquad (20)$$

$$S'(t) = \Lambda - \beta IS - \mu S, \qquad (21)$$

$$I'(t) = \beta IS - (\mu + \gamma)I, \qquad (22)$$

$$R'(t) = \gamma I - \mu R, \qquad (23)$$

where Λ is the birth rate, μ is the natural death rate and the rest of the parmeters are the same as the previous model [34].

The rate of change in the total population, N, is given by:

$$N'(t) = \Lambda - \mu N. \qquad (24)$$

The solution to this equation is:

$$N(t) = N_0 e^{-\mu t} + \frac{\Lambda}{\mu}(1 - e^{-\mu t}). \qquad (25)$$

The population size is therefore not constant, but is asymptomatically constant, with $N(t) \to \frac{\Lambda}{\mu}$ as $t \to \infty$.

The incidence rate is the number of transmissions for a unit of time, given by:

$$Incidence\ Rate = \beta IS. \qquad (26)$$

The basic reproduction number can be found by taking the susceptible population as $S = \frac{\Lambda}{\mu}$, as this would be the long term susceptible population, and by taking the infected population as $I = 1$. Substituting these values into equation 26 gives an incidence rate of:

$$Incidence\ Rate = \beta \frac{\Lambda}{\mu}. \qquad (27)$$

The average time that a person is infective for is:

$$Time\ Infected = \frac{1}{\gamma + \mu}. \qquad (28)$$

Therefore, if a single infective individual is placed into a susceptible population, the number of secondary infections, and hence the basic reproduction number, will be:

$$\mathcal{R}_0 = Time\ Infected \times Inicdence\ Rate = \frac{\Lambda\beta}{\mu(\mu + \gamma)}. \qquad (29)$$

There are two equilibrium points that can be found by setting the rate of change for equations 21, 22 and 23 to 0.

$$\Lambda - \beta IS - \mu S = 0, \qquad (30)$$

$$\beta IS - (\mu + \gamma)I = 0, \qquad (31)$$

$$\gamma I - \mu R = 0. \qquad (32)$$

Equation 31 gives two equilibrium conditions, one where the population is disease free and $I = 0$ and another endemic condition when $\beta S = \gamma + \mu$. By solving for these conditions, the disease free and endemic equilibriums can be obtained.

Disease free equilibrium:

$$\mathcal{E}_0 = \left(\frac{\Lambda}{\mu}, 0, 0\right). \quad (33)$$

Endemic equilibrium:

$$\mathcal{E} = \left(\frac{\Lambda}{\mu\mathcal{R}_0}, \quad \frac{\mu}{\beta}(\mathcal{R}_0 - 1), \quad \frac{\gamma}{\beta}(\mathcal{R}_0 - 1)\right). \quad (34)$$

The endemic equilibrium will only exist if $\mathcal{R}_0 > 1$.

As equations 21 and 22 are independent of equation 23, the following two-dimensional system can be used to analyse the stability of the equilibria:

$$\frac{dS}{dt} = \Lambda - \beta IS - \mu S, \quad (35)$$

$$\frac{dI}{dt} = \beta IS - (\mu + \gamma)I, \quad (36)$$

where $R = N - S - I$. The system is autonomous since the coefficients do not vary with time. The system can be nondimensionalized in order to simplify it and reduce the number of parameters, making analysis easier. This is done by substituting the independent and dependent variables with dimensionless quantities.

Tables 1 and 2 show the units of the endemic SIR models parameters and variables.

Table 1.

Parameter	Meaning	Unit
β	Rate of Infection	$\frac{people}{time}$
γ	Rate of Recovery	$time^{-1}$
μ	Death Rate	$time^{-1}$
Λ	Birth Rate	$\frac{people}{time}$

Table 2.

Variable	Meaning	Unit
N	Total Population	$people$
S	Susceptible Population	$people$
I	Infected Population	$people$
t	Time	$time$

Both the death rate, μ, and the rate of recovery, γ, have the units of time^{-1}. A new parameter, τ, can be defined as $\tau = (\gamma + \mu)t$ in order to obtain a dimensionless quantity. Let $S(t) = S\left(\frac{\tau}{\gamma+\mu}\right) = \hat{S}(\tau)$ and $I(t) = I\left(\frac{\tau}{\gamma+\mu}\right) = \hat{I}(\tau)$. The equations for $\frac{d\hat{S}}{d\tau}$ and $\frac{d\hat{I}}{d\tau}$ can be obtained by using the chain rule:

$$\frac{d\hat{S}}{d\tau} = \frac{dS}{dt} \times \frac{dt}{d\tau} = \frac{dS}{dt} \times \frac{1}{\gamma + \mu} = \frac{\Lambda - \beta IS - \mu S}{\gamma + \mu}, \quad (37)$$

$$\frac{d\hat{I}}{d\tau} = \frac{dI}{dt} \times \frac{dt}{d\tau} = \frac{dI}{dt} \times \frac{1}{\gamma + \mu} = \frac{\beta IS}{\gamma + \mu} - I. \quad (38)$$

The variables S and I are then rescaled using the total limiting population size. Substituting in $x(t) = \frac{\mu \hat{S}}{\Lambda}$ and $y(t) = \frac{\mu \hat{I}}{\Lambda}$ gives:

$$x' = \frac{\mu}{\Lambda} \times \frac{\Lambda - \beta y\left(\frac{\Lambda}{\mu}\right) x\left(\frac{\Lambda}{\mu}\right) - \mu x\left(\frac{\Lambda}{\mu}\right)}{\gamma + \mu} = \frac{\mu - \beta y x\left(\frac{\Lambda}{\mu}\right) - \mu x}{\gamma + \mu} = \rho(1 - x) - \mathcal{R}_0 xy, \qquad (39)$$

$$y' = \frac{\mu}{\Lambda} \times \left(\frac{\beta y\left(\frac{\Lambda}{\mu}\right) x\left(\frac{\Lambda}{\mu}\right)}{\gamma + \mu} - y\left(\frac{\Lambda}{\mu}\right) \right) = \frac{\beta y x\left(\frac{\Lambda}{\mu}\right)}{\gamma + \mu} - y = (\mathcal{R}_0 x - 1)y, \qquad (40)$$

where

$$\rho = \frac{\mu}{\gamma + \mu}. \qquad (41)$$

The five original parameters have been reduced to two dimensionless ones. The equilibria for the dimensionless SIR model can be found by setting equations 39 and 40 to 0:

$$x' = \rho(1 - x) - \mathcal{R}_0 xy = 0, \qquad (42)$$

$$y' = (\mathcal{R}_0 x - 1)y = 0. \qquad (43)$$

Again there are two equilibriums, the disease free equilibrium where $y = 0$ and $x = 1$, and the endemic equilibrium, where $x = 1/\mathcal{R}_0$ and $y = \rho(1 - 1/\mathcal{R}_0)$. The endemic equilibrium only exists if $\mathcal{R}_0 > 1$ as the boundary of the feasible region is $x \geq 0, y \geq 0$.

Dimensionless disease free equilibrium

$$\mathcal{E}_0 = (1,0). \qquad (44)$$

Dimensionless endemic equilibrium

$$\mathcal{E} = \left(\frac{1}{\mathcal{R}_0}, \rho\left(1 - \frac{1}{\mathcal{R}_0}\right) \right). \qquad (45)$$

The stability of the equilibria can be found by using the Jacobian matrix:

$$J(x, y) = \begin{bmatrix} -\rho - \mathcal{R}_0 y & -\mathcal{R}_0 x \\ \mathcal{R}_0 y & \mathcal{R}_0 x - 1 \end{bmatrix}. \qquad (46)$$

The Jacobian matrix for the disease free equilibrium is:

$$J(1,0) = \begin{bmatrix} -\rho & -\mathcal{R}_0 \\ 0 & \mathcal{R}_0 - 1 \end{bmatrix}, \qquad (47)$$

giving eigenvalues of:

$$\lambda_1 = -\rho, \qquad (48) \quad \lambda_2 = \mathcal{R}_0 - 1. \qquad (49)$$

Since this is an upper triangular matrix, the diagonal entries are the eigenvalues. If $\mathcal{R}_0 < 1$, then both eigenvalues are negative indicating the the equilibrium is a stable node. If $\mathcal{R}_0 > 1$, then λ_2 will be positive, indicating that the point is now an unstable saddle point.

The Jacobian matrix for the endemic equilibrium is:

$$J\left(\frac{1}{\mathcal{R}_0}, \rho\left(1-\frac{1}{\mathcal{R}_0}\right)\right) = \begin{bmatrix} -\mathcal{R}_0\rho & -1 \\ \mathcal{R}_0\rho - \rho & 0 \end{bmatrix}, \qquad (50)$$

giving eigenvalues of:

$$\lambda_{1,2} = \frac{-\rho\mathcal{R}_0 \pm \sqrt{(\rho\mathcal{R}_0)^2 - 4(\rho\mathcal{R}_0 - \rho)}}{2}. \qquad (51)$$

These two eigenvalues are in the form of the quadratic equation. If the dicriminant, Δ, is positive, then the two eigenvalues are real and negative, indicating that it is a stable node. If the disciminant is negative, then the eigenvalues are both complex congugate with a negative real part, indicating that it is a stable focus. If it is a stable focus, the system will tend to the endemic equilibrium through damped oscillations. An equation for the time period of these oscillations can be found. The infectious period is much shorter than the average lifespan. Therefore $\gamma \gg \mu$ and $\rho \approx 0$, meaning $\rho^2$is small enough to be neglected from calculations.

$$\lambda_{1,2} = -\frac{\rho\mathcal{R}_0}{2} \pm i\sqrt{\rho\mathcal{R}_0 - \rho} = -\xi \pm \eta j. \qquad (52)$$

If the eigenvalues of the jacobian are complex conjugates, the solution of the linearized system will be of the form $Ce^{-\xi\tau}\cos(\eta\tau + \phi)$, where C and ϕ are constants determined by the intial conditions [34]. Thus the system oscillates with the period T_{period} of:

$$T_{period} = \frac{2\pi}{\sqrt{\rho(\mathcal{R}_0 - 1)}}. \qquad (53)$$

The direction of flow in the system can found by using nullclines. The x-nullclines are where $x' = 0$. for this system there is one x-nullcline:

$$y = \frac{\rho}{\mathcal{R}_0}\frac{1-x}{x}. \qquad (54)$$

All vectors along an x-nullcline are parallel to the y axis and point either straight up or down. The direction can be found by subbing the value of y given by equation 54 into equation 40. If the sign of y' is positive, then the vector points upwards, if it is negative it points downwards.

$$y' = (\mathcal{R}_0 x - 1)\frac{\rho}{\mathcal{R}_0}\frac{1-x}{x}. \qquad (55)$$

If $x > \frac{1}{\mathcal{R}_0}$ then $y' > 0$, indicating that the vector arrow will point upwards. If $x < \frac{1}{\mathcal{R}_0}$, then $y' < 0$, indicating that the vector arrow will point downwards.

The y-nullclines exist where $y' = 0$. This gives two y-nullclines of:

$$y = 0, \qquad (56) \qquad x = \frac{1}{\mathcal{R}_0}. \qquad (57)$$

All vectors along a y-nullcline are parallel to the x axis and point either left or right. The direction can be found by subbing these values into equation 39. If the sign of x' is positive, then the vector points upwards, if it is negative it points downwards.

If $y = 0$:

$$x' = \rho(1 - x). \qquad (58)$$

Therefore if $x < 1$, then $x' > 0$ and the vector will point right. If $x > 1$, then $x' < 0$ and the vector will point left.

If $x = \frac{1}{\mathcal{R}_0}$:

$$x' = \rho\left(1 - \frac{1}{\mathcal{R}_0}\right) - y. \qquad (59)$$

Therefore if $y < \rho\left(1 - \frac{1}{\mathcal{R}_0}\right)$, then $x' > 0$ and the vector will point right. If $y > \rho\left(1 - \frac{1}{\mathcal{R}_0}\right)$, then $x' < 0$ and the vector will point left.

As the number of infective individuals at the endemic equilibrium is related to $\mathcal{R}_0$, it is possible to draw a forward bifurcation diagram with with the number of infective individuals at the equilibrium, y^*, as a function of $\mathcal{R}_0$. This is forward bifurcation as the endemic equibirium bifurcates as $\mathcal{R}_0$ increases and only exists for $\mathcal{R}_0 > 1$. The stable equibria for this system is given by:

$$y^* = \begin{cases} 0 & \mathcal{R}_0 < 1 \\ \rho\left(1 - \frac{1}{\mathcal{R}_0}\right) & \mathcal{R}_0 > 1. \end{cases} \qquad (60)$$

The disease free equilibrium at $y^* = 0$ also exists for $\mathcal{R}_0 > 1$, but is unstable.

Fitting Data

Realistic equation parameters can be calculated by using real world data. First, initial estimates for the parameters are obtained and used to produce an initial solution. The following two equations can be used to approximate initial values for the epidemic SIR model from available data:

$$mean\ time\ infected = \frac{1}{\gamma}, \qquad (61) \qquad \frac{\beta}{\gamma} = \frac{\ln\frac{S_0}{S_\infty}}{S_0 + I_{0-}S_\infty}, \qquad (62)$$

where S_∞ is the susceptible population at the end of the epidemic or the final size of the epidemic value.

This curve is then fitted to follow the data points as closely as possible by adjusting these parameter values. This is done by calculating the sum of squares error (SSE):

$$SSE = \sum_{i=1}^{n} (x_i - \hat{x}_i)^2, \qquad (63)$$

where x_i is the real world data value, $\hat{x}_i$ is the value estimated by the equations and n is the number of data points used. The function fminsearch uses the SSE function and the initial guesses for the parameters to perform unconstrained, nonlinear optimization of the function, and returns adjusted

parameter values that reduce the value of the SSE [31]. This process can be repeated until the SSE is no longer reduced. The parameter values obtained can then be used to plot a new curve that closely follows the real world data. One problem with this method is that different initial estimates may result in different final parameter and SSE values. Multiple sets of initial parameters may need to be used to find the smallest possible SSE [25]. The function lsqcurvefit can also be used to solve nonlinear least square problems. The function uses the same method of calculating the SSE and returning the parameter values that give the smallest error [32].

Avian Influenza Model

Avian influenza is currently only known to be transmitted to humans via contact with infected birds. Therefore it is important to understand how the virus behaves within bird populations. For this project avian influenza will be modelled using a set of SIRSI equations, with three equations representing the susceptible, infected and removed bird populations and two equations representing the susceptible and infected human populations:

$$S_b'(t) = \Lambda_b - \beta_b S_b I_b - \mu_b S_b, \qquad (64)$$

$$I_b'(t) = \beta_b S_b I_b - (\mu_b + \nu_b) I_b, \qquad (65)$$

$$R_b'(t) = \nu_b I_b - \mu_b R_b\,, \qquad (66)$$

where S_b is the susceptible bird population, I_b is the infected bird population, R_b is the removed bird population, Λ_b is the recruitment rate, β_b is the infection rate between birds, ν_b is the death rate due to avian influenza and μ_b is the natural death rate. The total poultry population is $N_b = S_b + I_b + R_b$.

$$S'(t) = \Lambda - \beta S I_b - \mu S, \qquad (67)$$

$$I'(t) = \beta S I_b - (\mu + \nu) I, \qquad (68)$$

where S is the susceptible bird population, I is the infected bird population, Λ is the recruitment rate, β is the infection rate between bird and humans, μ is the natural death rate of humans and ν is the death rate due to avian influenza.

Equations 64, 65 and 66 are independent of equations 67 and 68 and correspond to equations 21, 22 and 23 of the endemic SIR model. The analysis of the endemic SIR equations also applies to these three equations. Using the same process used to obtain equation 29, the reproduction number within the bird population is found to be:

$$\mathcal{R}_b = \frac{\Lambda_b \beta_b}{\mu_b(\mu_b + \nu_b)}. \qquad (69)$$

By setting equations 64, 65, 66, 67 and 68 to 0 it is found that there are two equilibrium conditions. One where the poultry population is infection free and $I_b = 0$ and another endemic condition when $\beta_b S_b = \nu_b + \mu_b$. By solving for these conditions, disease free and endemic equilibriums can be obtained.

Disease free equilibrium:

$$\mathcal{E}_0 = \left(\frac{\Lambda_b}{\mu_b}, 0, 0, \frac{\Lambda}{\mu}, 0\right). \qquad (70)$$

Endemic Equilibrium:

$$\mathcal{E} = (S_b^*,\ I_b^*, R_b^*, S^*, I^*\ ), \qquad (71)$$

where

$$S_b{}^* = \frac{(\mu_b + \nu_b)}{\beta_b}, \qquad (72) \qquad I_b{}^* = \frac{\mu_b}{\beta_b}(\mathcal{R}_b - 1), \qquad (73) \qquad R_b = \frac{\nu_b}{\beta_b}(\mathcal{R}_b - 1), \qquad (74)$$

$$S^* = \frac{\Lambda}{\beta\, I_b{}^* + \mu}, \qquad (75) \qquad I^* = \frac{\beta S^*\, I_b{}^*}{\mu + \nu}, \qquad (76)$$

Equations 64 and 65 are independent of equation 66 and can be nondimensionalized using the same process used to obtain equations 39 and 40 to give the dimensionless system:

$$x_b{}' = \rho_b(1 - x_b) - \mathcal{R}_b x_b y_b, \qquad (77)$$

$$y_b{}' = (\mathcal{R}_b x_b - 1)y_b, \qquad (78)$$

where

$$\rho_b = \frac{\mu_b}{\nu_b + \mu_b}. \qquad (79)$$

These equations can be used to analyse the direction of the systems flow using nullclines as well as asses the stability of the disease free and endemic equilbria using Jacobian matrices. The stability analysis (see appendix 12 for working) gives the same results as the endemic SIR model, with the disease free equilibrium Jacobian matrix having eigenvalues of:

$$\lambda_1 = -\rho_b, \qquad (80) \qquad \lambda_2 = \mathcal{R}_b - 1, \qquad (81)$$

This indicates that it is globally stable when $\mathcal{R}_b < 1$ as both eigenvalues will be negative, and unstable when $\mathcal{R}_b > 1$ as λ_2 will be positive. The endemic equilibrium Jacobian matrix has the eigenvalues of:

$$\lambda_{1,2} = \frac{-\rho_b\mathcal{R}_b \pm \sqrt{(\rho_b\mathcal{R}_b)^2 - 4(\rho_b\mathcal{R}_b - \rho_b)}}{2}, \qquad (82)$$

Indicating that the endemic equilibrium is globally stable when $\mathcal{R}_b > 1$, a stable node when the discriminant, Δ_b, is positive and a stable focus when Δ_b is negative. The forward bifurcation diagram can also be created for this system by plotting the equilibrium infected population $y_b{}^*$ against $\mathcal{R}_b$:

$$y_b{}^* = \begin{cases} 0 & \mathcal{R}_b < 1 \\ \rho_b\left(1 - \dfrac{1}{\mathcal{R}_b}\right) & \mathcal{R}_b > 1. \end{cases} \qquad (83)$$

Using the same process used to find the endemic SIR nullclines, the y-nullclines are:

$$y_b = 0, \qquad (84) \qquad x_b = \frac{1}{\mathcal{R}_b}. \qquad (85)$$

And the x-nullcline is:

$$y_b = \frac{\rho_b}{\mathcal{R}_b}\frac{1 - x_b}{x_b}. \qquad (86)$$

Real world data for human cases will be used to fit the unknown parameters of the bird-to-bird transmission rate, the bird-to-human transmission rate as well as the size of the initial infected bird population. The rest of the parameters will be given appropriate fixed values based on the available information about avian influenza.

7. Project Progress and Results

Lotka-Volterra Model

A Lotka-Volterra model was created using MATLAB (see appendix 3) in order to understand the systems behaviour.

The solid lines in figure 1 show the solutions to the Lotka-Volterra equations (equations 1 and 2) using the parameter and initial values given in tables 3 and 4. The equations give periodic solutions. Predator populations grow when there are large numbers of prey, but eventually fall as the prey populations decline due to hunting. When the predator populations are low, the prey population increases again. This cycle of growth and decline continues.

Figure 1.

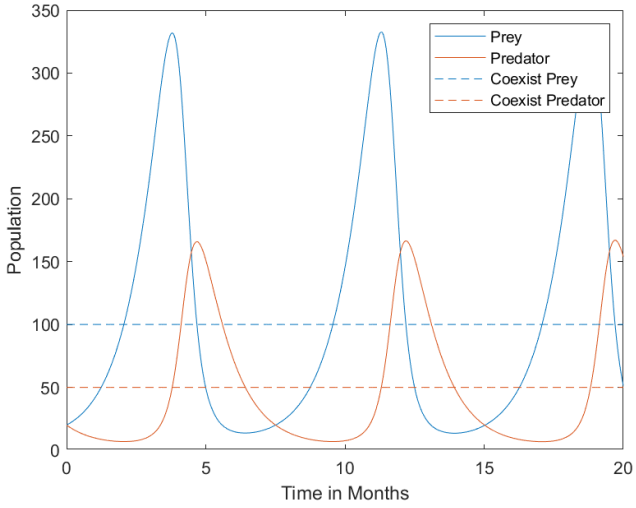

Figure 2.

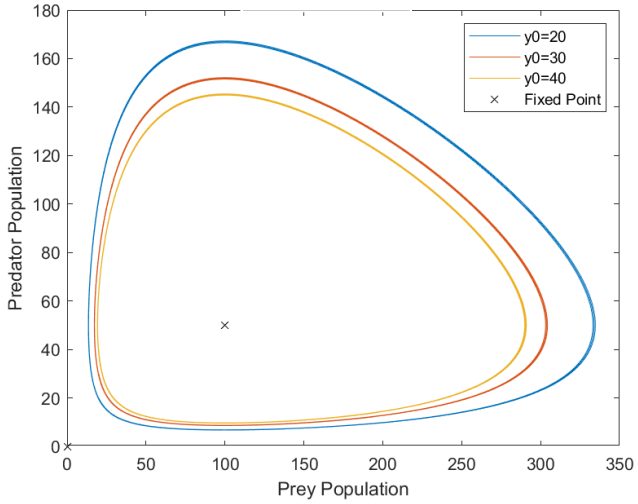

By using the same parameter values but changing the initial predator population value, the phase portrait showing prey population against predator population in figure 2 was obtained. Each trajectory is travelling anti-clockwise with time. There are two equilibrium points, the extinction equilibrium where both species would die out and the coexistence equilibrium where both populations remain constant as shown by the dashed lines in figure 1. From equations 3 and 4 the fixed points are:

$$E_0 = (0,0), \qquad E = \left(\frac{\gamma}{\delta}, \frac{\alpha}{\beta}\right) = \left(\frac{1}{0.1}, \frac{1}{0.2}\right) = (100, 50).$$

The phase portrait in figure 2 can be used to demonstrate the two fixed points of the system and their stability. The extinction equilibrium is a saddle point as shown by the eigenvalues in equations 7 and 8. As the prey population approaches zero, the predator population starts to rapidly decrease but never reaches zero. As the predator population approaches zero the prey population starts to rapidly increase. Both populations are both able to approach close to zero and still recover unless one of the populations is artificially changed to zero. If the prey population was changed to zero, the predator population would have no food and rapidly approach zero. If there were no predators, the prey population would continue to grow. Saddle points are unstable, if the fixed point was stable the populations would be attracted towards the extinction equilibrium. The eigenvalues for the coexistence equilibrium are complex and conjugate as shown by equations 10 and 11. This means the point is elliptic and solutions will oscillate around the fixed point, as shown in figure 2.

Table 3.

Parameter	Meaning	Value
α	Prey Growth Rate	1
β	Predation Rate	0.02
δ	Relationship between Prey Population Size and Predator Growth Rate	0.01
γ	Predator Natural Death/Emigration Rate	1

Table 4.

Initial Condition	Meaning	Value
x_0	Initial Prey Population	20
y_0	Initial Predator Population	20

SIR Epidemic Model

An SIR epidemic model was created using MATLAB (see appendix 4) in order to demonstrate the systems behaviour.

Figure 3 shows the solution to the epidemic SIR equations (equations 13, 14 and 15) using the parameters and initial values given in tables 5 and 6. The susceptible population is always declining until it reaches the final number of people that avoided the disease. The removed population continues to increase until it reaches the final number of removed individuals. The infected population is nonmonotonic, initially increasing to a peak before decreasing to zero. As the infected population doesn't immediately approach zero the basic reproduction number must be above 1.

Figure 3.

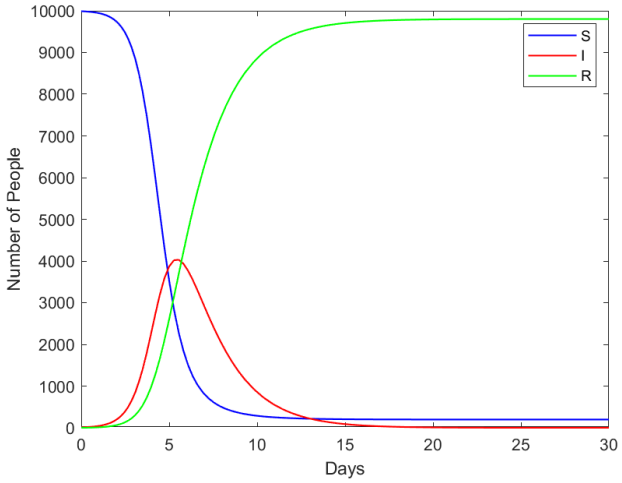

Figure 4.

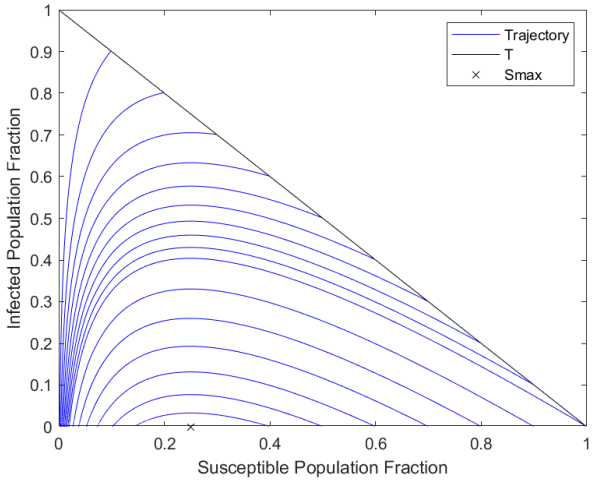

Using equation 19 we find $\mathcal{R}_0 = \frac{\beta S_0}{\gamma} = 3.996$. Since $\mathcal{R}_0 > 1$, there is an epidemic.

By changing the initial infected and removed populations the phase portrait showing the susceptible fraction of the population against the infected fraction of the population in figure 4 was obtained. The trajectories are flowing from right to left with time. As the infected population increases, the susceptible population increases. As people recover from the disease and enter the removed population, both the infected population and susceptible population decrease. However the infected population approaches zero at a much faster rate and the susceptible population will approach a nonzero final population of S_∞. The peak for the infected population is higher if there is a higher initial infected population, but lower if there is a higher fraction of the population in the removed population due to

immunity or vaccination. If the initial susceptible population fraction is smaller than S_{max}, then the infected population will immediately trend to zero. The triangle T is given by:

$$T = \{(s, i) | s \geq 0, i \geq 0, s + i \leq 1\}, \qquad (87)$$

where s is the susceptible population fraction and i is the infected population fraction. Solutions within the triangle are positively invariant and so do not leave the triangle and there are unique solutions for all positive time [28]. The model is well posed as the solutions behaviour changes continuously with the initial conditions. The maximum number of people infected at one time is given by equation 17. For the parameter values given in tables 5 and 6:

$$I_{max} = -\frac{\gamma}{\beta} + \frac{\gamma}{\beta}\ln\frac{\gamma}{\beta} + S_0 + I_0 - \frac{\gamma}{\beta}\ln S_0 = 4036.8.$$

This equation shows that the peak increases as the initial infected population is increased, and decreases as the initial removed population is increased, as this causes the initial susceptible population to decrease. The maximum number of susceptible people at the end of the epidemic, S_{max}, is given by equation 16:

$$S_{max} = \frac{\gamma}{\beta} = 2500.$$

Herd immunity, p, is achieved when the fraction for the removed population is:

$$p = 1 - \frac{1}{\mathcal{R}_0} = 0.75. \qquad (88)$$

Table 5.

Parameter	Meaning	Value
β	Rate of Infection	0.0002
γ	Rate of Recovery	0.5

Table 6.

Initial Condition	Meaning	Value
N	Total Population	10000
S_0	Initial Susceptible Population	9990
I_0	Initial Infected Population	10
R_0	Initial Recovered Population	0

SIR Endemic Model

An SIR endemic model was created using MATLAB (see appendix 5) in order to demonstrate the systems behaviour.

Figure 5 shows the solution to the endemic SIR equations (equations 21, 22 and 23) using the parameters and initial values for a hypothetical animal population given in tables 7 and 8. The susceptible population has a large initial decline as the disease first spreads through the population, before recovering slightly as more of the species is born, increasing the population that has not yet had the disease. There is a peak at around 1 year before the susceptible population declines again, due to more of the population being infected with the disease. There is then a peak around every

year, decreasing in amplitude, before the susceptible population reaches a steady state. The infective population initially increases quickly as the disease passes through the susceptible population. Then as the susceptible population declines the infective population also declines as there are less of the species for the infected animals to pass the disease onto. The infective population declines to a near zero level before recovering as the susceptible population increases as there are now more animals that can have the disease passed on to them. There are then peaks around a year apart until the infective population reaches a steady state. These peaks occur slightly after the susceptible populations peaks. The removed population initially increases as the infective population recovers, but then declines as those immune to the disease die due to other causes and are replaced by susceptible new-borns. The removed population reflects the changes in the susceptible population, growing as the susceptible population declines and decreasing as the susceptible population increases until both populations reach a steady state. As there is an endemic equilibrium and the disease remains in the population, $\mathcal{R}_0 > 1$.

Figure 5.

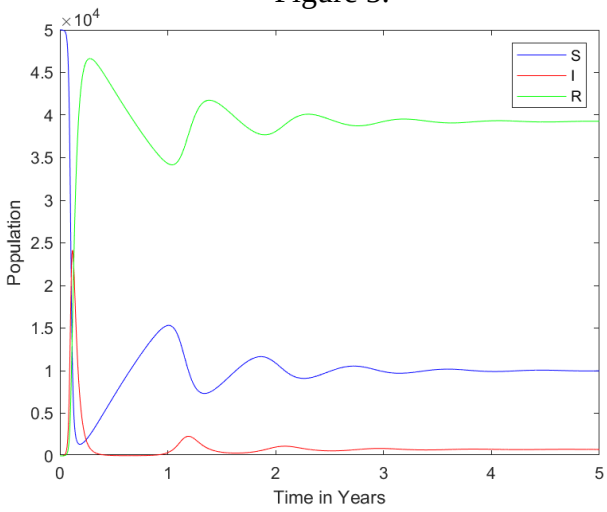

Figure 6.

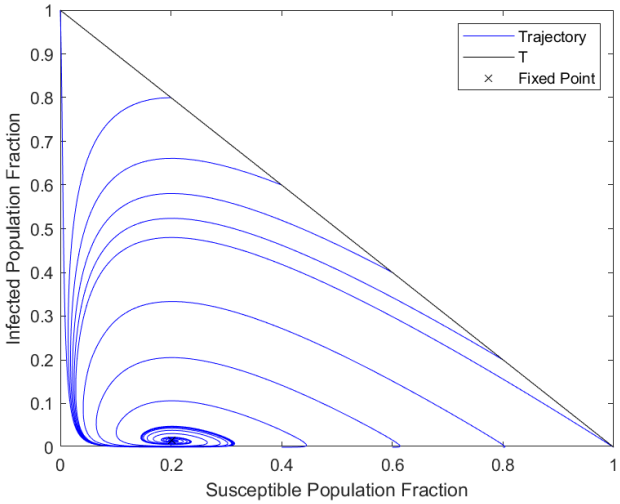

By changing the initial infected and removed populations, the phase portrait in figure 6 was obtained, showing the susceptible population fraction against the infected population fraction. All trajectories tend towards the endemic equilibrium fixed point. A majority of the trajectories move initially from right to left, with the proportion of the population that is infected increasing and the proportion of the population that is susceptible decreasing. The trajectories then hit a peak for the fraction of the population that is infected and decreases rapidly with little change in the susceptible population. The infected population then reaches near zero levels, and the susceptible population begins to increase as more susceptible animals are born and immune animals die. Once there are more susceptible animals for the disease to be passed on to, the infected population increases. The trajectory then begins to spiral around the fixed point, decreasing in size each oscillation, before reaching and remaining at the endemic equilibrium. The trajectories that started with susceptible population fractions of 0.6 and 0.4 initially had a small increase in the susceptible population, with the immune population dying and being replaced with susceptible new-borns, before the number of infected cases significantly rose. The trajectories that started with a large initial infected population immediately start to decrease to near zero levels before tending towards the endemic equilibrium. The phase portrait is bounded by triangle T, given by equation 87.

Using equation 29, the basic reproduction number for this system is given by:

$$\mathcal{R}_0 = \frac{\Lambda\beta}{\mu(\mu+\gamma)} = 5.$$

Therefore this is a endemic as $\mathcal{R}_0 > 1$ and the diesease will remain in the population.

Using equation 34, the endemic equilibrium is given by:

$$\mathcal{E} = \left(\frac{\Lambda}{\mu\mathcal{R}_0}, \quad \frac{\mu}{\beta}(\mathcal{R}_0 - 1), \quad \frac{\gamma}{\beta}(\mathcal{R}_0 - 1)\right)$$

$$= (10000, \quad 754.7, \quad 39245.3)\,.$$

Using equation 41, the dimensionless quantity ρ is given by:

$$\rho = \frac{\mu}{\mu+\gamma} = \frac{1}{53}.$$

Using equation 53, the approxiamtion for the oscillation time period is given by:

$$T_{period} = \frac{2\pi}{\sqrt{\rho(\mathcal{R}_0 - 1)}} = 22.871.$$

The equivalent time in years is given by:

$$t = \frac{\tau}{\mu+\gamma} = \frac{22.871}{0.5+26} = 0.863\ years.$$

As the peaks in the populations occur just under a year apart, this appears to be an accurate approxiamtion for the oscillation time period.

The type of equilibrium can be found by evaluating discriminant of the eigenvalues given by equation 51:

$$\Delta = (\rho\mathcal{R}_0)^2 - 4(\rho\mathcal{R}_0 - \rho) = -0.293.$$

As the discriminant is negative, the eigenvalues are complex conjugate with a negative real part, indicating that the fixed point is a stable focus and not a stable node.

Table 7.

Parameter	Meaning	Value
β	Rate of Infection	0.00265
γ	Rate of Recovery	26
μ	Death Rate	0.5
Λ	Birth Rate	25000
ρ	Dimensionless Prameter	1/53

Table 8.

Initial Condition	Meaning	Value
N	Total Population	50000
S_0	Initial Susceptible Population	49999
I_0	Initial Infected Population	1
R_0	Initial Recovered Population	0

Figure 7 shows the the solution to the endemic SIR equations using the same parameters as before, except for the rate of infection which is now $\beta = 4.77 \times 10^{-4}$, giving a basic reproduction number of $\mathcal{R}_0 = 0.9$, and the initial conditions have been changed to $S_0 = 40000$ and $I_0 = 10000$. The

infected population monotonically decreases to 0, as the infected animals infect on average less than 1 other animal before recovering. The susceptible population intially sees a decrease as the disease passes through the population, but quickly recovers as the infected population goes down and new susceptible animals are born. The removed population intially increases as the infected animals recover, but then decreases as the immune animals die of natural causes and are not replaced as there are no new infections. The phase portrait in figure 8 was obtained by changing the intial infected and susceptible populations. All of the trajectories monotonically decrease to zero infections as more animals are recovering from the disease than there are new infections. The susceptible populations then increase as the immune animals die and are replaced with susceptible new-borns until the trajectories reach the disease free equilibrium where there are no infections and the population is completely susceptible.

Figure 7.

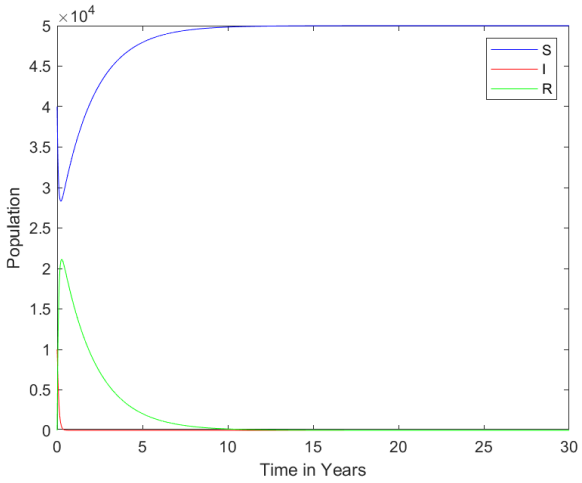

Figure 8.

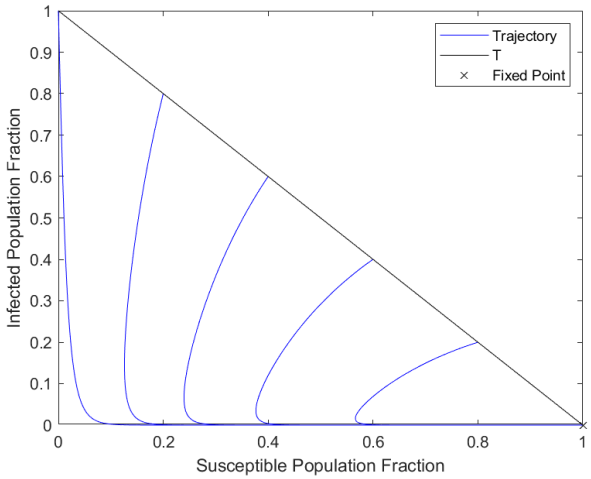

Figure 9 and 10 show the nullclines for the two previous endemic models with the $\mathcal{R}_0$ values of 5 and 0.9 respectively. For the two phase planes there are only solutions in the region $x \geq 0$, $y \geq 0$, $x + y \leq 1$. The y-nullclines indicate where $y' = 0$, and therefore there is only a change in the x value at any point along the nullclines. The x-nullclines indicate where $x' = 0$, and therefore there is only a change in the y value at any point along these nullclines. The intersections of an x-nullcline and a y-nullcline indicate where both $x' = 0$ and $y' = 0$. Hence any intersections are equilibrium points. The arrows indicate the direction of the tangent vectors along the nullclines and how trajectories will flow in neighbouring regions bounded by the x-nullcline and y-nullcline. In figure 9 it can be seen that there are two intersections, at the endemic equilibrium and the disease free equilibrium. It is shown that any trajectory will flow around the endemic equilibrium and away from the disease free equilibrium, except if the y value is forced to 0. This indicates that the endemic equilibrium is either a centre, node or focus and that the disease free equilibrium is a saddle point. It also shows that if a trajectory starts to the right of the vertical y-nullcline and above the x-nullcline, then the trajectory will travel upwards and to the left. Therefore for these trajectories there will be a peak y value at $x = 1/\mathcal{R}_0$. If the trjactory starts to the left of the vertical y-nullcline, then the infected population will immediately begin to decrease before flowing around the endemic equilibrium.

In figure 10 it can be seen that there is only one intersection in the feasibe region, the disease free equilibrium. It is shown that any trajectory will flow towards it, indicating that it is a stable node. It

also shows that if a trajectory begins above the x-nullcline, then the trajectory will travel to the left and downwards, with the minimum number of animals in the susceptible fraction at $y = \frac{\rho}{\mathcal{R}_0}\frac{1-x}{x}$. The trajectory will then flow downwards and to the right, travelling towards the disease free equilibrium. As long as the initial y value is non-zero, the number of animals infected will decrease no matter where the trajectory begins. Both of the nullcline plots confirm the qualitive behaviour of the phase plane trajectories demonstrated in the phase portraits shown in figures 6 and 8.

Figure 9.

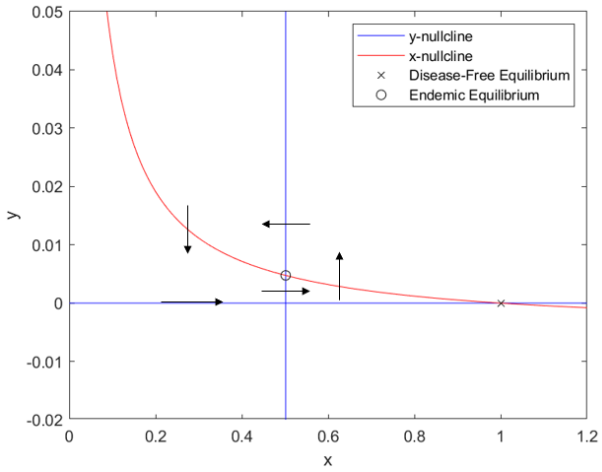

Figure 10.

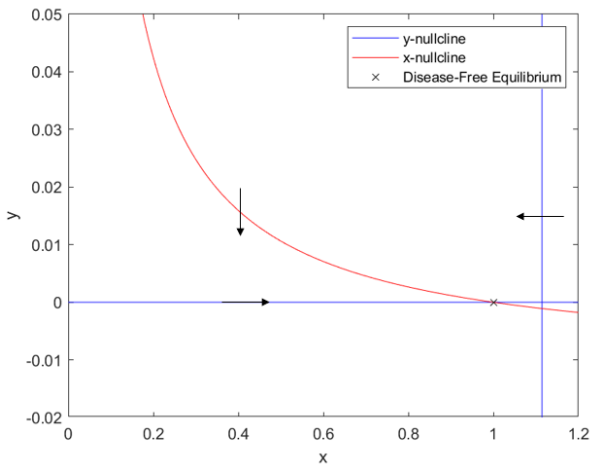

Figure 11 shows the forward bifurcation diagram for the parameter values given in table 7, and how the dimensionless quantity corresponding to the equilibrium level of infective animals, y^*, changes with $\mathcal{R}_0$. The solid line indicates that the equilibrium is stable and the dashed line indicates that the equilibrium is unstable. It is shown that the disease free equilibrium is globally stable for $\mathcal{R}_0 < 1$ and unstable for $\mathcal{R}_0 > 1$. The stable endemic equilibrium arises from the bifurcation point $\mathcal{R}_0 = 1$ and increases in size as $\mathcal{R}_0$ increases, with $y^* \to \rho$ as $\mathcal{R}_0 \to \infty$. The endemic equilibrium only exists for $\mathcal{R}_0 > 1$, whereas the disease free equilibrium exists for all values of $\mathcal{R}_0$. This is a transcritical bifurcation as the stability of the disease free equilibirum changes after the birfurcation point.

Figure 11.

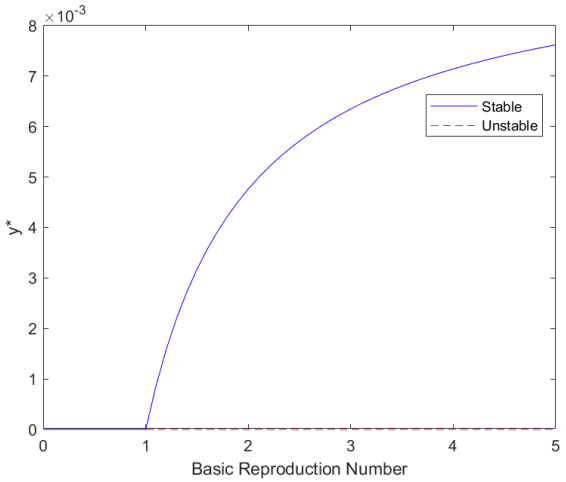

Fitting Graphs to Data

A model that fits SIR equations (equations 13, 14 and 15) to data was created using MATLAB (see appendix 6) in order to understand how real world data can be used to adjust parameters. The model used data from an influenza outbreak in a boarding school during 1978 and is based on the information and model from Martcheva [25]. The school housed 763 boys, 19 of which were not infected by the illness. The data available for the epidemic is displayed in table 9.

Table 9.

Day	Number of Cases	Day	Number of Cases
3	25	9	192
4	75	10	126
5	227	11	71
6	296	12	28
7	258	13	11
8	236	14	7

To fit the curve initial estimates for the parameters were first obtained. The mean time that the students were infected for was 3 days. Using equation 26 and days as the units for time infected, the rate of recovery can be estimated:

$$\gamma = \frac{1}{mean\ time\ infected} \approx 0.3.$$

A value for the rate of transmission can be obtained using equation 27, the rate of recovery, the values from the data of $S_3 = 738$, $I_3 = 25$ and $S_\infty = 19$:

$$\beta = \gamma \times \frac{\ln \frac{S_3}{S_\infty}}{S_3 + I_3 - S_\infty} \approx 0.0025.$$

These parameters were used to estimate the solution for the infected population in figure 12. For this solution the SSE is 72000. After optimization the new values for the parameters obtained were $\alpha = 0.465$ and $\beta = 0.00237$. The solution for the infected population with these new parameters is shown in figure 13 and has an SSE value of 4000.

Figure 12.

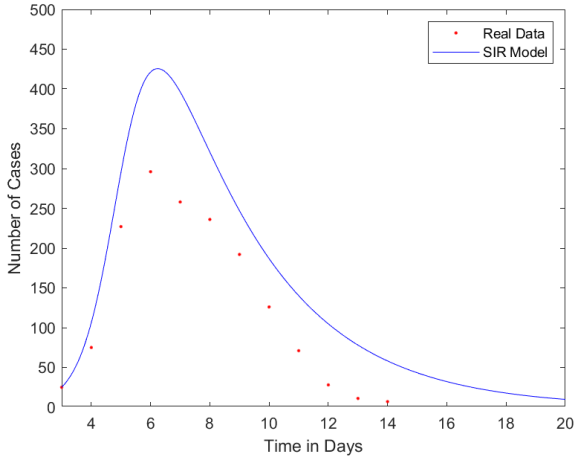

Figure 13.

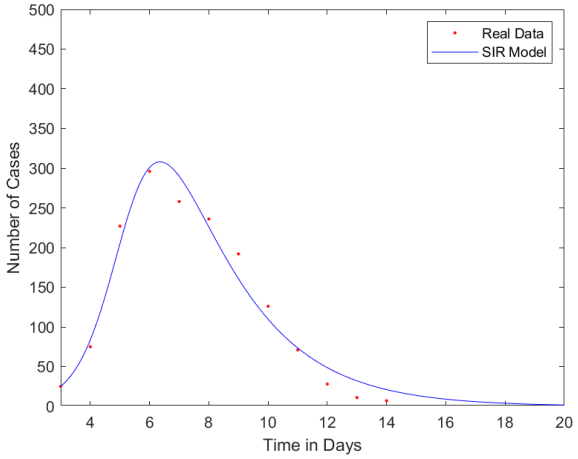

Avian Influenza Model

A model was created that fits the parameters for the avian influenza SIRSI equations (equations 64, 65, 66, 67 and 68) using real world data for H5N1 human cases (see appendix 7). Data for human cases was obtained from the WHO database [14]. This model is based on the information available and model from Martcheva [26].

Some of the parameters for this model were possible to predetermine and fix. The average population between 2005 and 2020 for the 17 countries that have had human bird cases were calculated and totalled to provide a value for the total human population. The average number of poultry units over the 15 year period for each country were calculated and totalled to provide a total bird population. Statistics for the populations and number of poultry units in each country is available from the Food and Agriculture Organization of the United Nations (FAO) [27]. If units are too small or too large the round off errors may be too big and affect the fit. Therefore for this model the human population uses units of 10^5 and the poultry population uses units of 10^6.

The values for the other parameters were calculated as follows:

- The mean lifespan for poultry is taken to be 2 years, giving the natural death rate for the bird population as $\mu_b = 0.5 years^{-1}$.
- The total population is assumed to remain constant, which means $\frac{\Lambda_b}{\mu_b}$ = total bird population.
- The mean infectious period for birds is taken as 10 days, giving $\nu_b = 36.5 years^{-1}$ as the avian influenza induced death rate.
- The average human lifespan is taken to be 65 years, giving a natural death rate of $\mu = \frac{1}{65} years^{-1}$.
- The total human population is assumed to be constant, and so $\frac{\Lambda}{\mu}$ = total human population.
- The initial infected human population is estimated to be 50.

All these parameters are fixed, leaving the initial infected bird population, transmission coefficient between poultry and transmission coefficient between birds and humans to be fitted. The fixed parameter values and initial conditions as well as the initial estimates for the values to be fitted are shown in tables 10 and 11.

The parameters will be fitted by comparing the cumulative number of human cases predicted by the model to the real world data. The cumulative number of human cases, $I_{cumulative}$, is taken as the solution to the following equation:

$$I_{cumulative}{}'(t) = \beta S I_b, \qquad (89)$$

The MATLAB function lsqcurvefit returns the outputs resnorm and residual. Residual is a column matrix of the residual differences between each of the real data points and the models solution, and resnorm is the squared 2-norm of the residual. This means $resnorm = residual^T residual$, returning a single value. This value will be taken as the fits error and used to compare the different models.

Using information from Martcheva [26] as well an estimate of $\mathcal{R}_b = 1.5$, the initial estimates are:

$$\beta_b = \frac{\mathcal{R}_b \mu_b (\mu_b + \nu_b)}{\Lambda_b} \approx 0.003, \qquad \beta = 10^{-8}, \qquad I_b(0) = 5.$$

Figure 14.

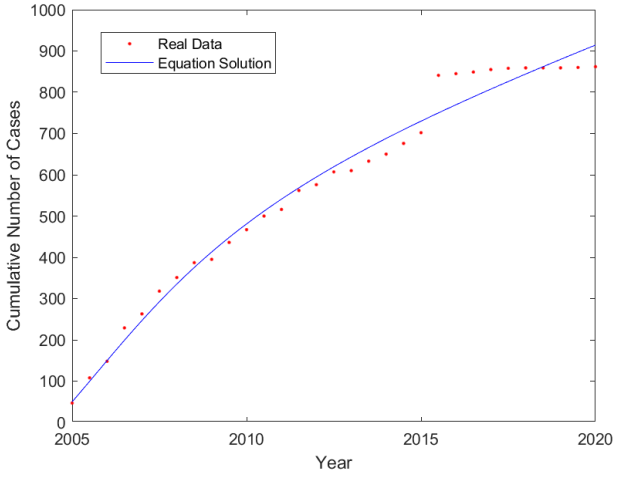

Figure 15.

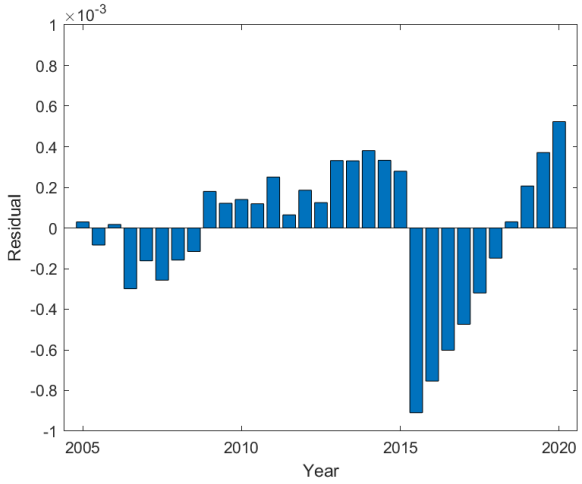

$$\beta_b = 0.00224264, \quad \beta = 2.03812 \times 10^{-8}, \quad I_b(0) = 1.81519, \quad \mathcal{R}_b = 1.00252,$$

$$error = 3.541 \times 10^{-6}.$$

Figure 14 shows the models solution and the real world data. Suitability of the model can be assessed by plotting the residuals, as shown in figure 15. If it is a suitable model for the given data the residuals should be small and random. This model has quite large residuals concentrated around 2015, and therefore may be unsuitable. In 2015 Egypt reported 136 human cases, the largest by a single country in a single year. The WHO claimed this was not due to any changes in the virus itself, but due to a large number of localised poultry infections, insufficient awareness, behavioural patterns and inadequate precautions taken when handling poultry [33]. Therefore these human cases could be treated as an anomaly and removed from the data when trying to see the dynamics of the disease in the poultry population. Using the same parameter estimates as before gives the solution in figure 16:

Figure 16.

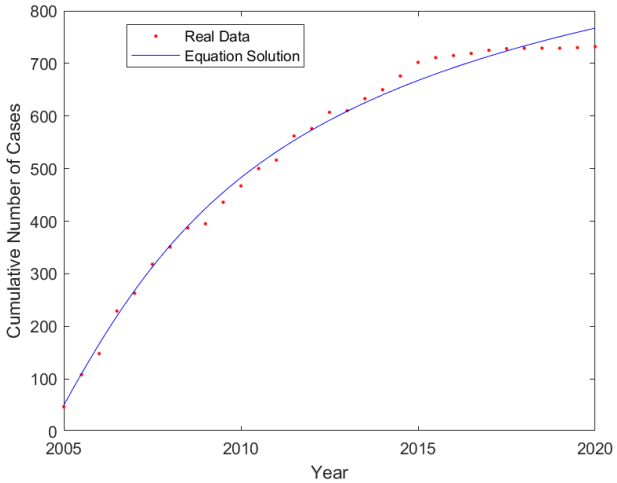

Figure 17.

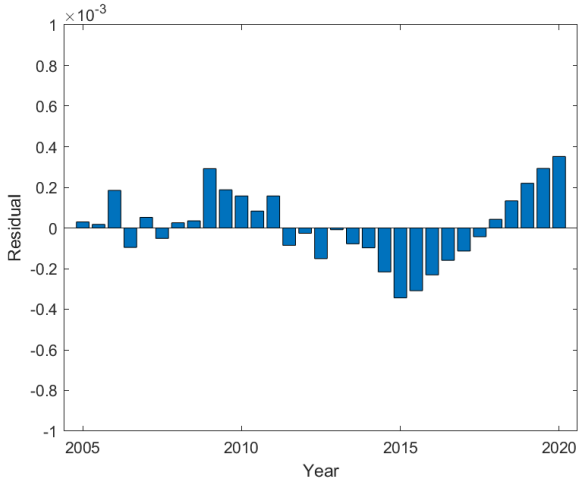

$$\beta_b = 0.00223379, \quad \beta = 3.36031 \times 10^{-8}, \quad I_b(0) = 1.37375, \quad \mathcal{R}_b = 0.998564,$$

$$error = 9.0754 \times 10^{-7}.$$

Removing the anomaly reduces the error significantly, however the residuals shown in figure 17 are still not random, and so this model may still not be appropriate. The large outbreak in 2015 is followed by only 15 human cases between 2016 to 2020. It is possible that this small number of cases is due to

more awareness of the disease and better precautions being taken by poultry farmers rather than an actual change in the dynamics of the disease in the poultry populations. The system of equations is able to model the data from 2005 to 2015 very closely, and so another option would be to use only this group of data to fit the parameters and understand the diseases behaviour. The solution could then be extrapolated to 2020 to see how the prediction compares to the unused real world data. Using the same initial parameter estimates as before gives the solution shown in figure 19:

Figure 19.

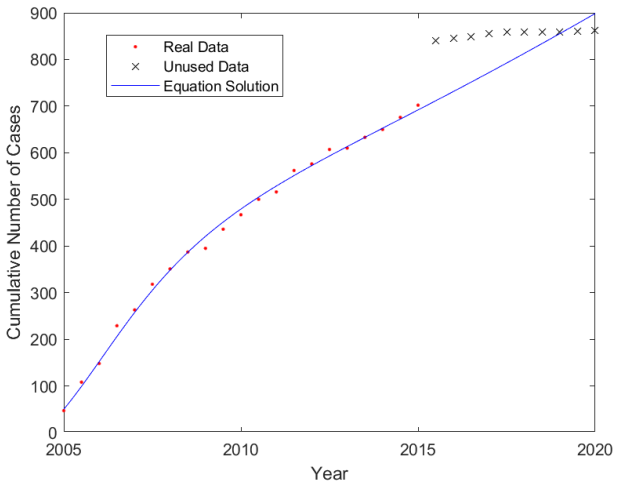

Figure 20.

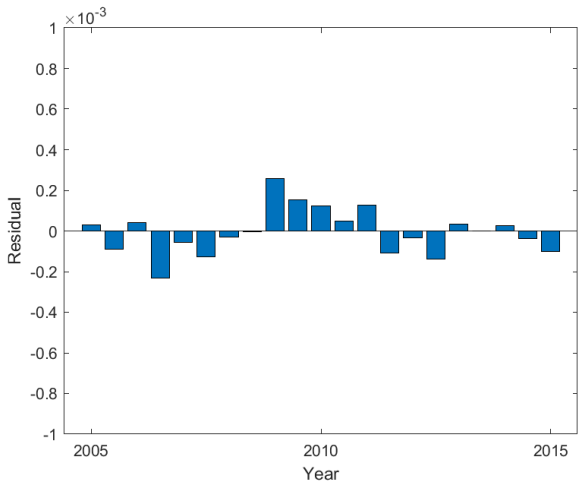

$$\beta_b = 0.00225678, \quad \beta = 8.57079 \times 10^{-9}, \quad I_b(0) = 4.06552, \quad \mathcal{R}_b = 1.00884,$$

$$error = 2.539 \times 10^{-7}.$$

There are 21 data points from 2005 to 2015, therefore to compare this model to the other two models only the error from the first 21 residuals should be considered. The first and second model give errors of 9.794×10^{-7} and 4.409×10^{-7} respectively. This model has less error than the other two and the residuals shown in figure 20 are more random, and therefore it is taken as the best model for avian influenzas dynamics and will be used to plot the final results. The extrapolation of the solution to 2020 is only slightly larger than the real world data, showing that this model is biologically feasible.

Using different initial parameter estimates can have an impact on the final parameter values as well as the error of the fit. The initial estimates were changed incrementally and their impact on the final results were observed (see appendix 11 for the values of the initial parameter estimates tested). Of the tested initial estimates, the output parameter values that gave the smallest error were found to be:

$$\beta_b = 0.002244137005728, \quad \beta = 1.53792 \times 10^{-8}, \quad I_b(0) = 2.54309696071527,$$

$$\mathcal{R}_b = 1.00318989391202, \quad error = 2.350 \times 10^{-7}.$$

Figure 21 shows the solution using these parameters extrapolated to the year 2035. It closely follows the real world cases in 2020 showing that this model is feasible, with further extrapolation predicting that there will be around 1275 human cases by the year 2035. Figure 22 shows how the infected bird population changes over time. There is a very small initial increase from 2.55 million to 2.63 million as birds are being infected at a faster rate than they are dying. The infected bird population then starts to decrease as the rate infected birds die overtakes the rate they are able to infect other birds due to the decrease in the susceptible birds to spread the disease to. The population continues to decrease towards the endemic equilibrium at a slowing rate. The rate slows as the number of susceptible birds recovers

and therefore there are more birds to pass the disease onto. At the endemic equilibrium, infected birds are spreading the disease to susceptible birds at the same rate that infected birds are dying, causing the infected population size to remain constant. This model predicts that it will take until around 2030 for the infective bird population to reach the endemic equilibrium of 700 thousand birds, which is biologically feasible.

Figure 21.

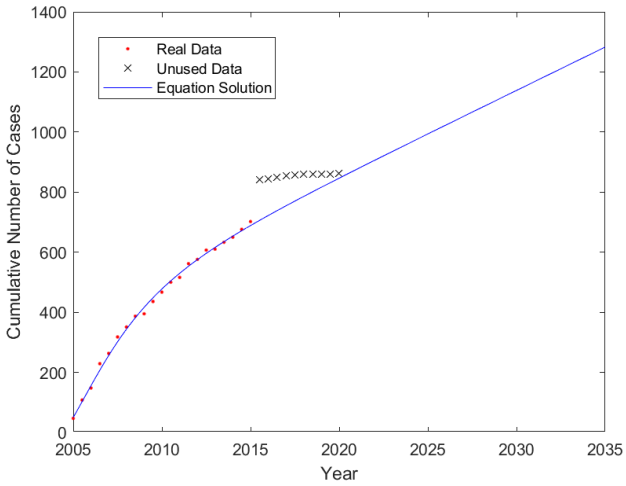

Figure 22.

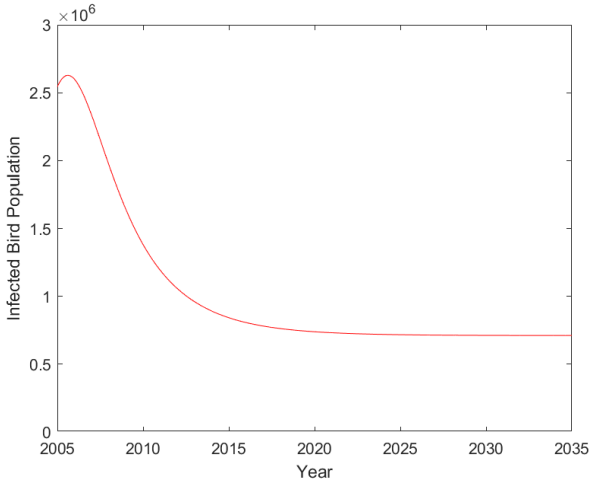

Figure 23 shows how the susceptible bird population changes with time. It initially decreases rapidly as the disease spreads through the population, before recovering as new susceptible birds are recruited at a faster rate than the infected birds can pass on the disease until it reaches the endemic equilibrium. At the endemic equilibrium, susceptible birds are being infected and dying of natural causes at the same rate that new susceptible birds are being recruited, keeping the population size constant. Figure 24 shows the phase plane plot of the susceptible bird population against the infective bird population. The trajectory initially starts are the top travelling left to right over time, with the susceptible population initially decreasing and the infected population seeing a slight increase, peaking at 2.63 million, before decreasing as the rate at which infected birds die overtakes the rate of new infections. The susceptible population reaches its lowest value of 16.405×10^9 then starts to increase again as the rate that new susceptible birds are recruited is higher than the rate at which birds are being infected, whilst the infective population continues to decrease. This continues until both populations reach the endemic equilibrium.

Figure 23.

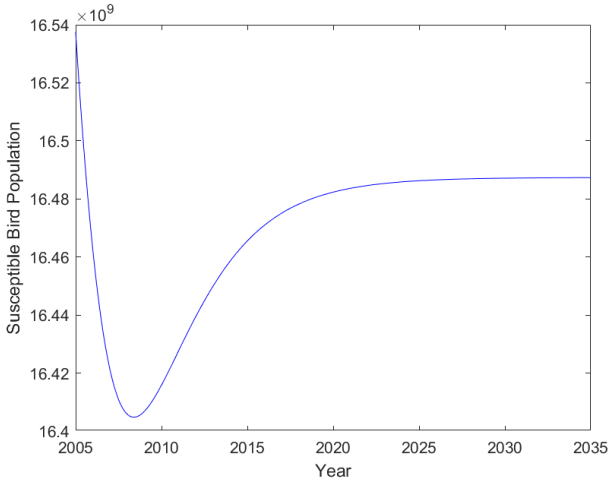

Figure 24.

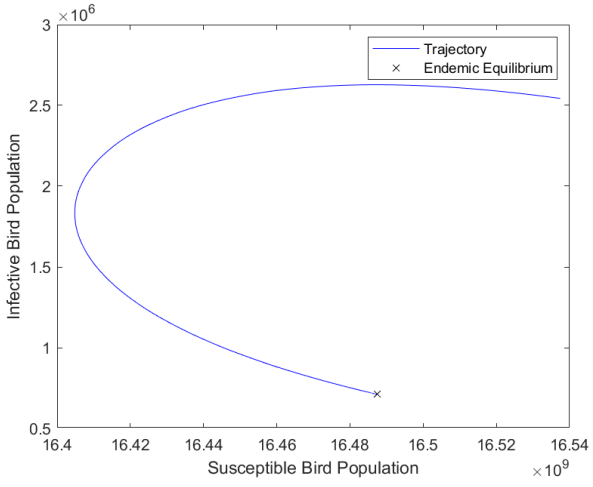

Figure 25 shows how the removed bird population changes with time. It initially sees an increase as the large initial infected population dies, peaking at around 135 million, but then decreases towards the endemic equilibrium, as the rate new susceptible birds are recruited overtakes the rate at which birds are infected and die from the disease. The replacement of the dead birds with newly recruited birds causes the susceptible population to grow and the removed population to shrink. The removed curve is qualitatively a reflection of the susceptible curve. At the equilibrium, birds are dying from avian influenza at the same rate new susceptible birds are being recruited, therefore the removed population remains constant at around 53 million birds. Figure 26 shows the total poultry deaths due to avian influenza, calculated using the equation:

$$R_{b\_cumulutive}{}'(t) = \nu_b I_b{}^*. \qquad (90)$$

It estimates around 720 million birds have died in the past 15 years due to avian influenza in the effected countries, and predicts around another 380 million will die by 2035. The overall bird population in these countries is around 16.5 billion, and so this number is feasible.

Figure 25.

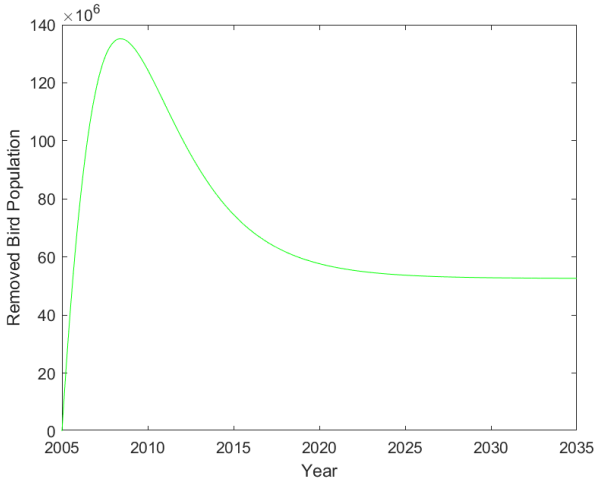

Figure 26.

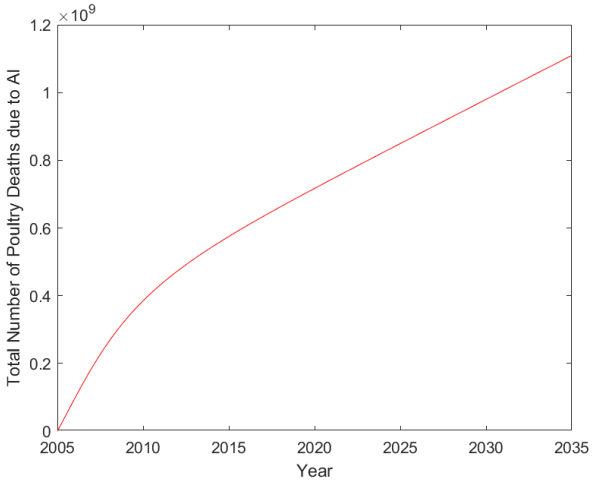

The endemic equilibrium is given by $\mathcal{E} = (S_b{}^*,\ I_b{}^*, R_b{}^*, S^*, I^*)$, where

$$S_b{}^* = \frac{(\mu_b + \nu_b)}{\beta_b} = 16487.4, \quad I_b{}^* = \frac{\mu_b}{\beta_b}(\mathcal{R}_b - 1) = 0.710717, \quad R_b{}^* = \frac{\nu_b}{\beta_b}(\mathcal{R}_b - 1) = 51.882,$$

$$S^* = \frac{\Lambda}{\beta\, I_b{}^* + \mu} = 2.63670, \quad I^* = \frac{\beta S^*\, I_b{}^*}{\mu + \nu} = 7.893 \times 10^{-6}.$$

This model predicts that at the endemic equilibrium there will be around 710 thousand infected birds, 16.487 billion susceptible birds, 51.9 million birds in the removed population and 0.79 infected humans. These numbers are biologically feasible and demonstrate that the curves shown in figures 22, 23 and 25 follow the expected behaviour. By substituting the endemic equilibrium values into equations 89 and 90, the number of human cases each year and the number of birds that die due to avian influenza each year are:

$$I_{cumulative}{}'(t) = \beta S^* I_b{}^* = 2.882 \times 10^{-4}, \qquad R_{b\_cumulative}{}'(t) = \nu_b I_b{}^* = 25.941.$$

It predicts that at the equilibrium point there will be around 29 new human cases a year and around 25.9 million birds dying due to avian influenza each year. Both of these values are biologically feasible.

The eigenvalues of the endemic equilibriums Jacobian matrix are given by equation 82. The discriminant, Δ_b, of the of the eigenvalue indicates what type of equilibrium the endemic equilibrium is. Using equation 79 gives $\rho_b = 1/74$, therefore the discriminant is:

$$\Delta_b = (\rho_b \mathcal{R}_b)^2 - 4(\rho_b \mathcal{R}_b - \rho_b) = 1.136 \times 10^{-5}.$$

As the discrimant is positive, the eigenvalues are negative and real, indicating that the endemic equilibrium is a stable node. This is shown by the trajectory in figure 24 flowing towards the endemic equilibrium without oscillating around it.

Figure 27.

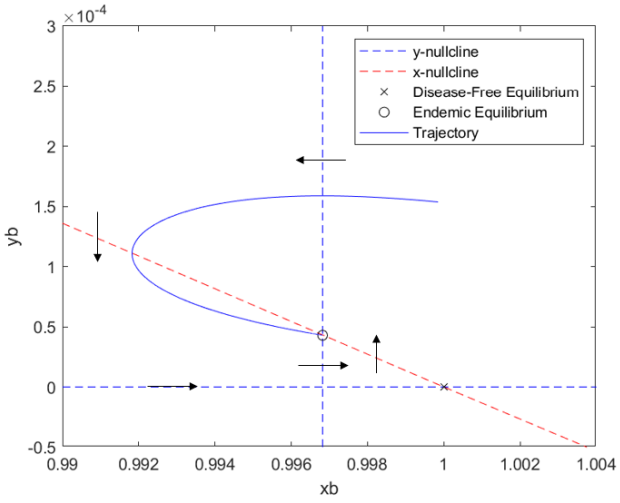

Figure 28.

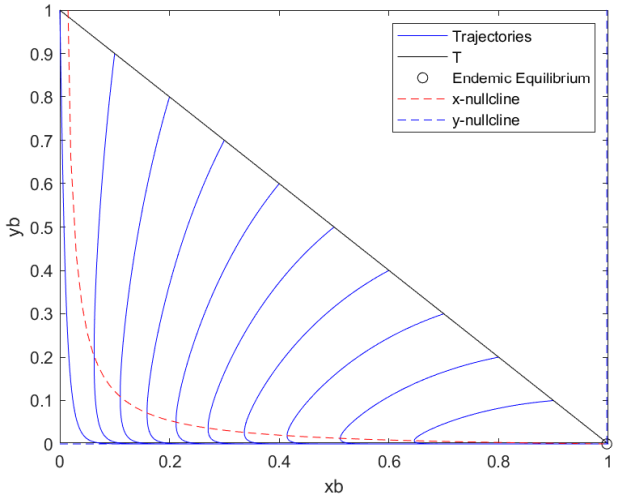

Figure 27 shows the nullclines for the avian influenza model and the phase plane plot of the dimensionless susceptible and infective poultry populations. These are similar to the endemic SIR model nullclines shown in figure 9. For the phase plane there are only solutions in the region $x_b \geq 0$, $y_b \geq 0$, $x_b + y_b \leq 1$. The two intersections of the x and y-nullclines are the endemic equilibrium and the disease free equilibrium. The arrows indicate the direction of the tangent vectors along the nullclines and how trajectories will flow in neighbouring regions bounded by the x-nullcline and y-nullcline. It is shown that any trajectory will flow around the endemic equilibrium and away from the disease free equilibrium, except if the y_b value is forced to 0. This indicates that the disease free equilibrium is an unstable saddle point and that the endemic equilibrium is either a centre, node or focus. It also shows that if a trajectory starts to the right of the vertical y-nullcline and above the x-nullcline, then the trajectory will travel upwards and to the left. Therefore for these trajectories there will be a peak y_b value at $x_b = 1/\mathcal{R}_b$. These trajectories will also travel left and reach the minimum x_b value at the x-nullcline, $y_b = \frac{\rho_b}{\mathcal{R}_b}\frac{1-x_b}{x_b}$. This behaviour is shown by the plotted trajectory, flowing initially from right to left, with y_b peaking at $x_b = 1/\mathcal{R}_0$ before flowing left and downwards until it reaches the x-nullcline where it starts to travel to the right and downwards until it reaches the endemic equilibrium without oscillating around it, indicating that this fixed point is a stable node.

By changing the initial conditions the phase portrait in figure 28 was created. The trajectories to the right of the x-nullcline are moving to the left as the susceptible population decreases due to disease spreading through the population and downwards as the infected birds are dying quicker than they are infecting other birds. The trajectories to the left of the x-nullcline are flowing to the right as new susceptible birds are being recruited quicker than the susceptible population is being infected and the trajectory also flows downwards as the infected population continues to decrease. This flow continues

until the trajectories reach the endemic equilibrium. These trajectories confirm what is shown by the directions of the nullcline tangent vectors in figure 27.

Figure 29.

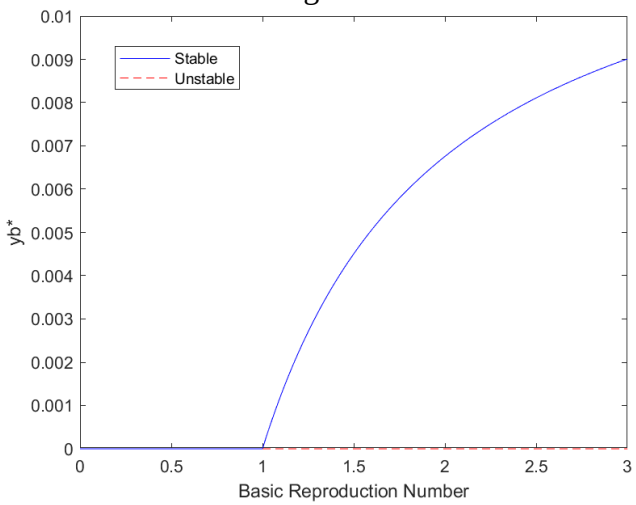

Figure 30.

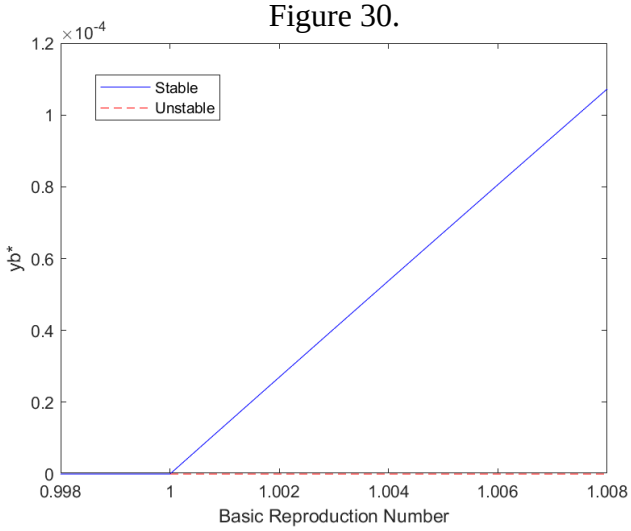

Figures 29 and 30 are forward bifurcation diagrams for the avian influenza model. Figure 29 shows the impact the disease mutating to have a larger transmission coefficient could have on the size of the infected bird population at the endemic equilibrium. For example, if avian influenza had a basic reproduction number of 2, the endemic infective population would be $y_b{}^* \approx 0.007$, which corresponds to around 116 million birds. Figure 30 shows the same forward bifurcation diagram over a smaller range. This shows the impact a small change in the fitted parameter values could have on the size of the endemic equilibrium infected population. For example, if the fitted parameters give $\mathcal{R}_b = 1.002$, then $y_b{}^* \approx 0.00025$ which corresponds to 4 million birds. If the parameters give a value of $\mathcal{R}_b = 1.004$, then $y_b{}^* \approx 0.0005$ which corresponds to 8 million birds.

Limitations of the avian influenza model:

- Assumes that the transmission coefficients are constant and the same for every country. It is likely that human behaviour and poultry farm conditions change over time and between countries. Seasonality also has an impact with changing temperatures impacting the transmission of the disease.
- Assumes constant and closed human and poultry populations. In reality both populations will change in size over time and there will be movement of people and poultry from other countries.
- Assumes the only source of the infection for poultry is other infected poultry. In reality there are external sources of avian influenza such as wild water fowl that are natural reservoirs for the disease.
- Does not take into account vaccinations of poultry, which is a method used to control the spread.
- Fits 3 parameters. More parameters being fitted decreases the accuracy of the model.
- Small changes in the initial parameter estimates impacts the final parameter values.
- Only considers poultry populations in countries with human cases.
- The fixed parameter estimations may be inaccurate.
- Small sample size of human cases to fit data to. Easy for anomalies to impact the final results.
- Assumes the country the individual was infected in is same as the country they were diagnosed in. They may have been infected whilst visiting another country.

Table 10.

Parameter	Meaning	Value
Λ_b	Poultry recruitment rate	8270
μ_b	Poultry natural death rate	0.5
ν_b	Poultry death rate due to avian influenza	36.5
β_b	Poultry-poultry transmission coefficient initial estimate	0.003
Λ	Human birth rate	26370/65
μ	Human natural death rate	1/65
ν	Human death rate due to avian influenza	36.5
β	Poultry-human transmission coefficient initial estimate	10^{-8}

Table 11.

Initial Conditions	Meaning	Value
N_b	Total poultry population	16540
S_{b0}	Initial susceptible population	16535
I_{b0}	Initial infective poultry population estimate	5
R_{b0}	Initial removed poultry population	0
S_0	Initial susceptible human population	26370
I_0	Initial infected human population	0.0005

8. Conclusion

In conclusion, the project has been a success. The aim of this project was to create a model that demonstrated the dynamics of avian influenza based on previous outbreaks, and this has been achieved. This project first looked at the simpler nonlinear systems of Lotka-Volterra equations, before moving onto the more complex epidemic and endemic SIR equations. This helped to develop a good understanding of the behaviour of nonlinear systems and gain an appreciation of how the ODE systems could be modelled using the MATLAB software. It was found that the models created followed the expected theory. The project then looked at how real world data can be used to find suitable values for parameters and initial conditions. This technique was used to fit the parameters for an avian influenza model using the data available for the H5N1 strain. An SIRSI model then used the parameter values to simulate and study the nonlinear dynamics of avian influenza in human and bird populations.

The final Gannt chart is shown in appendix 1. The initial literature review took longer than expected as there was difficulty finding a suitable avian influenza model to build upon that was both simple enough to understand and used real world data. Through thorough research and guidance from the project supervisor, an appropriate model was eventually found. There were also disruptions due to university technical issues causing deadlines for other modules to be changed, impacting the time originally intended for project work. The schedule also changed due to the understanding of the subject area improving and gaining a better knowledge of what was achievable during the available time frame.

Although the objectives of this project have been completed there is still further work that could be done to improve the model:

- The current model assumes that transmission coefficients are constant over time, when in reality they will change due to seasonality and changes in human behaviour. A nonautonomous model where the two transmission coefficients are functions of time could be used.
- A vaccinated poultry class could be included to show the control measure impacts the dynamics of avian influenza.
- Elasticity analysis of the models parameters could be implemented by changing the parameter values by 1% and observing the impact on the output solution. This would help assess the effectiveness of different control measures by considering which parameters they impact.

This further work would contribute to improving the understanding of the nonlinear dynamics of avian influenza.

References

[1] B. Mishra and D. Sinha, 'Mathematical Model on Avian Influenza with Quarantine and Vaccination', *Journal of Immunological Techniques in Infectious Diseases*, vol. 05, Jan. 2016.

[2] J. Zhang, Y. Li, Z. Jin, and H. Zhu, 'Dynamics Analysis of an Avian Influenza A (H7N9) Epidemic Model with Vaccination and Seasonality', *Complexity*, Mar. 17, 2019.

[3] S. Liu, L. Pang, S. Ruan, and X. Zhang, 'Global Dynamics of Avian Influenza Epidemic Models with Psychological Effect', *Computational and Mathematical Methods in Medicine*, Mar. 12, 2015. https://www.hindawi.com/journals/cmmm/2015/913726/ (accessed Nov. 12, 2020).

[4] A. D.j and B. I.h, 'History of highly pathogenic avian influenza', vol. 28, no. 1, pp. 19–38, Apr. 2009.

[5] CDC, 'Avian Influenza in Birds | Avian Influenza (Flu)', Nov. 19, 2018. [Online]. Available: https://www.cdc.gov/flu/avianflu/avian-in-birds.htm (accessed Nov. 10, 2020).

[6] H. K. Leong *et al.*, 'Prevention and Control of Avian Influenza in Singapore', vol. 37, no. 6, p. 6, 2008.

[7] R. Alders, J. A. Awuni, B. Bagnol, P. Farrell, and N. de Haan, 'Impact of avian influenza on village poultry production globally', *Ecohealth*, vol. 11, no. 1, pp. 63–72, 2014.

[8] K.Dhama, A. Kimar *et al*, 'Avian/Bird Flu Virus: Poultry Pathogen Havving Zoonotic and Pandemic threats: A Review', *Journal of Medical Sciences*, Vol. 13, pp. 301-315, July 2013.

[9] A. McLeod, N. Morgan *et al*, 'Economic and Social Impacts of Avian Influenza', FAO Emergency Centre for Transboundary Animal Diseases Operations, Geneva, 2005.

[10] E. Shim and A. P. Galvani, 'Evolutionary Repercussions of Avian Culling on Host Resistance and Influenza Virulence', *PLoS One*, vol. 4, no. 5, May 2009.

[11] CDC, 'CDC - AVIAN INFLUENZA - NIOSH Workplace Safety and Health Topic', Oct. 17, 2018. [Online]. Available: https://www.cdc.gov/niosh/topics/avianflu/default.html (accessed Nov. 13, 2020).

[12] WHO, 'WHO | No bird flu risk for consumers from properly cooked poultry and eggs', Dec. 2005. [Online]. Available: https://www.who.int/mediacentre/news/releases/2005/pr66/en/ (accessed Nov. 13, 2020).

[13] D. Mackenzie, 'Deadly H5N1 may be brewing in cats', *New Scientist*. [Online]. Available: https://www.newscientist.com/article/mg19325883-800-deadly-h5n1-may-be-brewing-in-cats/ (accessed Nov. 13, 2020).

[14] WHO, 'Cumulative number of confirmed human cases for avian influenza A(H5N1) reported to WHO, 2003-2020', Jan. 2020. [Online]. Available: https://www.who.int/influenza/human_animal_interface/2020_01_20_tableH5N1.pdf?ua=1 (accessed Nov. 13, 2020).

[15] CIDRAP , 'Five Koreans had H5N1 virus but no illness', Sep. 2006. [Online]. Available: https://www.cidrap.umn.edu/news-perspective/2006/09/five-koreans-had-h5n1-virus-no-illness (accessed Nov. 13, 2020).

[16] M. Smallman-Raynor and A. D. Cliff, ‘Avian Influenza A (H5N1) Age Distribution in Humans’, *Emerg Infect Dis*, vol. 13, no. 3, pp. 510–512, Mar. 2007.

[17] OIE, ‘OIE expert mission finds live bird markets play a key role in poultry and human infections with influenza A(H7N9) : OIE - World Organisation for Animal Health’, Apr. 2013. [Online] Available: https://www.oie.int/en/for-the-media/press-releases/detail/article/oie-expert-mission-finds-live-bird-markets-play-a-key-role-in-poultry-and-human-infections-with-infl/ (accessed Nov. 13, 2020).

[18] European Centre for Disease Prevention and Control, ‘Novel avian influenza A(H7N9) virus outbreak’, Jan 2018. [Online]. Available: https://www.ecdc.europa.eu/en/avian-influenza-humans/threats-and-outbreaks/AH7N9-outbreak (accessed Nov. 13, 2020).

[19] L. Zhou, Q. Li, and T. M. Uyeki, ‘Estimated Incubation Period and Serial Interval for Human-to-Human Influenza A(H7N9) Virus Transmission,’ *Emerging Infectious Diseases journal - CDC*, vol. 25, no. 10, Oct. 2019.

[20] M. Martcheva, *An Introduction to Mathematical Epidemiology*. New York: Springer Science + Business Media, 2015.

[21] TIEM, ‘Predator - Prey DYNAMICS’. 1999. [Online]. Available: http://www.tiem.utk.edu/~gross/bioed/bealsmodules/predator-prey.html (accessed Nov. 13, 2020).

[22] A. MacLean, C. Celso, and M. Stumpf, ‘Stem Cell Population Biology: Insights from Haematopoiesis’, *Stem cells (Dayton, Ohio)*, vol. 35, Sep. 2016.

[23] R. Beckley, C. Weatherspoon, M. Alexander, M. Chandler, A. Johnson, and G. S. Bhatt, ‘Modeling Epidemics with Differential Equations’, June 2013. [Online]. Available: http://www.tnstate.edu/mathematics/mathreu/filesreu/GroupProjectSIR.pdf (accessed Nov. 13, 2020).

[24] R. K. Upadhyay, N. Kumari, and V. S. H. Rao, ‘Modeling the spread of bird flu and predicting outbreak diversity’, *Nonlinear Anal Real World Appl*, vol. 9, no. 4, pp. 1638–1648, Sep. 2008.

[25] M. Martcheva, ”Fitting models to data,” in *An Introduction to Mathematical Epidemiology*. New York: Springer Science + Business Media, 2015. pp. 126-130.

[26] M. Martcheva, ”Zoonotic Disease, Avian Influenza, and Nonautonomous Models,” in *An Introduction to Mathematical Epidemiology*. New York: Springer Science + Business Media, 2015. pp. 281-283.

[27] Food and Agriculture Organization of the United Nations. ‘FAOSTAT’, 2021. [Online]. Available: http://www.fao.org/faostat/en/#data (accessed Mar. 05, 2021).

[28] H. W. Hethcote, ‘The Mathematics of Infectious Diseases’, *SIAM Rev.*, vol. 42, no. 4, pp. 599–653, Jan. 2000, doi: 10.1137/S0036144500371907.

[29] Mathworks.‘Choose an ODE Solver - MATLAB & Simulink - MathWorks United Kingdom’, 2021. [Online] Available: https://uk.mathworks.com/help/matlab/math/choose-an-ode-solver.html (accessed Mar. 05, 2021).

[30] Mathworks. ‘Stiff Differential Equations’, 2021. [Online] Available: https://uk.mathworks.com/company/newsletters/articles/stiff-differential-equations.html (accessed Mar. 05, 2021).

[31] Mathworks. ‘Find minimum of unconstrained multivariable function using derivative-free method - MATLAB fminsearch - MathWorks United Kingdom’, 2021. [Online] Available: https://uk.mathworks.com/help/matlab/ref/fminsearch.html (accessed Mar. 05, 2021).

[32] Mathworks. ‘Solve nonlinear curve-fitting (data-fitting) problems in least-squares sense - MATLAB lsqcurvefit - MathWorks United Kingdom’, 2021. [Online] Available: https://uk.mathworks.com/help/optim/ug/lsqcurvefit.html (accessed Mar. 05, 2021).

[33] World Organisation for Animal Health, ‘Egypt: upsurge in H5N1 Human and Poultry Cases But No Change in Transmission Pattern of Infection’, 2015. [Online] Available: https://www.oie.int/en/egypt-upsurge-in-h5n1-human-and-poultry-cases-but-no-change-in-transmission-pattern-of-infection/ (accessed May 05, 2021).

[34] M. Martcheva, “The SIR Model with Demography: General Properties of Planar Systems,” in *An Introduction to Mathematical Epidemiology*. New York: Springer Science + Business Media, 2015. pp. 37-56.

Appendix 1 – Project Schedule (Gantt chart)

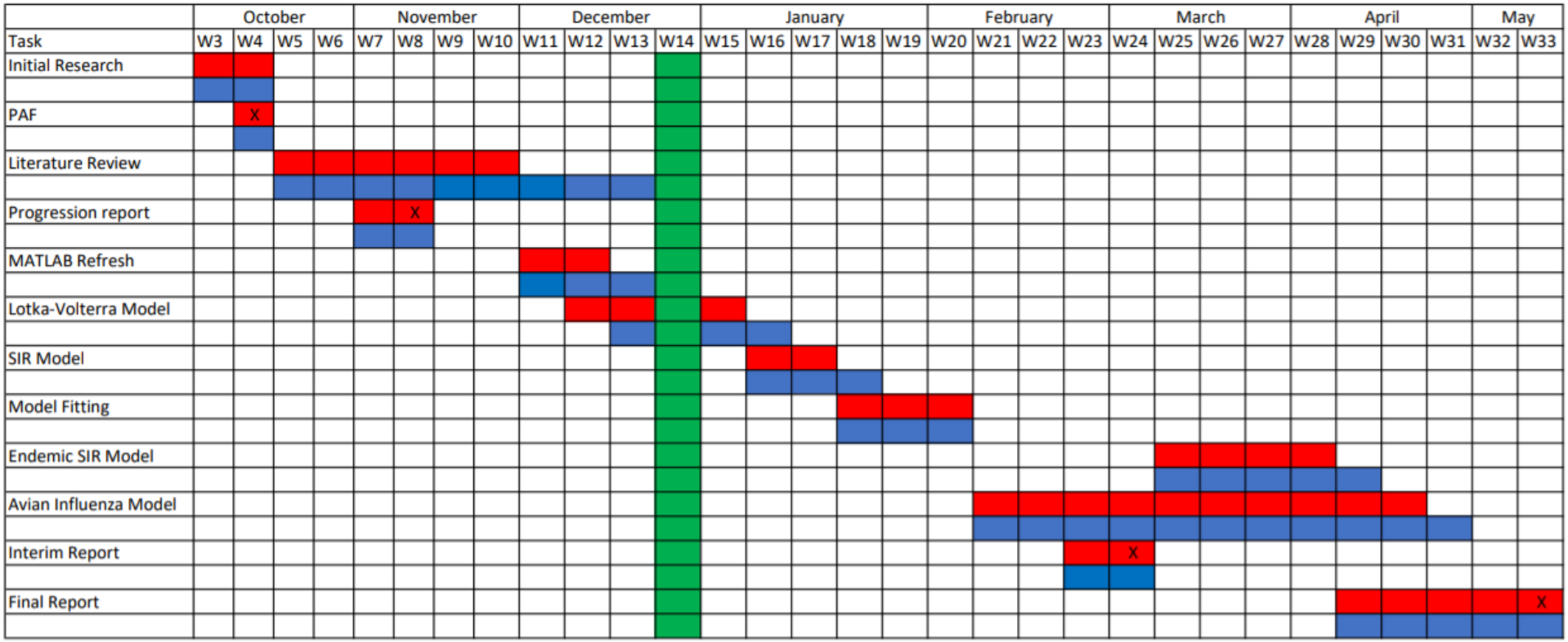

Appendix 2 – Cost Estimate

N/A

Appendix 3 – Lotka-Volterra Model Code

```
function dx = LV_plot(t, x)

function dx = LV(t, x)  % Lotka-Volterra equations

dx = [0; 0];     % assign zeros to dx
alpha = 1;       % prey growth rate
beta = .02;      % predation rate
delta = .01;     % relationship between prey population size
    ... and predator population growth
gamma = 1;       % predator natural death/migartion rate

dx(1) = - beta * x(1) * x(2) + x(1) * alpha ;  % rate of
change of
    ... prey population
dx(2) = x(2) * x(1) * delta - gamma * x(2); % rate of change
of
    ... predator population

end

y0 = 20;                    % inital predator population
x0 = 20;                    % initial prey population
tperiod = [0:0.01:15];      % time period

[t,x] = ode45(@LV, tperiod, [x0 y0]); % solve ODEs

subplot(1,2,1)          % subplot 1
plot(t,x)               % plot predator and prey populations
against time
hold on
xlabel('Time in Months'); ylabel('Population');   % label axis
legend('Prey','Predator');

for y0 = 20:10:40       % initial predator population values
    ... for phase plane

    [t,x] = ode45(@LV, tperiod, [x0 y0]); % solve ODEs

    subplot(1,2,2)          % subplot 2
    plot(x(:,1),x(:,2));    % plot prey population vs predator
population
    ... phase plane
    hold on

end
```

```
plot(100,50,'kx',0,0,'kx')       % plot fixed points
xlabel('Prey Population');       % label phase plane axis
ylabel('Predator Population');
legend('y0=20','y0=30','y0=40','Fixed Point');  % legend for
initial
    ... predator values

end
```

Appendix 4 – Epidemic SIR Model Code

```
function SIR_plot

N = 10000;                      % total population
tperiod = [0:0.01:35];          % time period
R0 = 0;                         % initial removed population
I0 = 10;                        % initial infected population
S0 = N-(I0+R0);                 % initial susceptible population

function dx = SIR(t, x)         % SIR ODEs

dx = [0; 0; 0];                % assigns zeroes to dx
beta = 0.0002;                 % rate of infection
gamma = 0.5;                   % rate of recovery

dx(1) = x(2) * x(1) * -beta;       % change in susceptible
population
dx(2) = x(2) * beta * x(1) - x(2) * gamma;    % change in
infected
   ...population
dx(3) = x(2) * gamma;              % change in removed
population

end

[t,x] = ode45(@SIR, tperiod, [S0 I0 R0]);       % solves ODE

subplot(1,2,1);
plot(t,x(:,1),'b',t,x(:,2),'r',t,x(:,3),'y');
    % plots susceptible, infected and removed populations
against time
xlabel('Days'); ylabel('Number of People');     % label axis
legend('S','I','R');
```

```
% for phase plane plot a range of initial condition values are
needed

for I0 = [10:1000:9010]     % initial infected populations for
phase plane

    S0 = N-(I0+R0);             % initial susceptible
population

    [t,x] = ode45(@SIR, tperiod, [S0 I0 R0]); % solves ODE

    SF = x(:,1)./N;             % susceptible population
fraction
    IF = x(:,2)./N;             % infected population fraction
    T=1-SF;                     % triangle indicating S + I <
1

    subplot(1,2,2);
    plot(SF,IF,'b',SF,T,'k','linewidth',.5); ylim([0 1]);   %
plot
    ... phase plane
    xlabel('Susceptible Population Fraction'); % label phase
plane
    ylabel('Infected Population Fraction');
    hold on
end

for R0 = 1000:1000:6000     % initial removed populations for
phase plane

I0 = 10;                    % initial infected population
S0 = N-(I0+R0);             % initial susceptible population

[t,x] = ode45(@SIR, tperiod, [S0 I0 R0]);   % solves ODE

SF = x(:,1)./N;             % susceptible population fraction
IF = x(:,2)./N;             % infected population fraction

subplot(1,2,2);
plot(SF,IF,'b','linewidth',.5)  % plot phase plane
hold on
end

end
```

Appendix 5 – Endemic SIR Model Code

```
function SIR_endemic_plot
```

```
format long

N = 50000;                          % total population
tperiod = [0:0.001:5];             % time period
R0 = 0;                             % initial removed population
I0 = 1;                             % initial infected population
S0 = N-(I0+R0);                     % initial susceptible
population

function dx = sir(t, x)             % SIR ODEs

dx = [0; 0; 0];                     % assigns zeroes to dx
beta = 0.00265;                    % rate of infection
gamma = 26;                         % rate of recovery
mu = 1/2;                           % natural death rate
N = 50000;                          % total population
lambda = N*mu;                      % birth rate


dx(1) = lambda - beta * x(1) * x(2) - mu * x(1);      % change
in
    ... susceptible population
dx(2) = beta * x(1) * x(2) - gamma * x(2) - mu * x(2);    %
change in
    ... infected population
dx(3) = gamma * x(2) - mu * x(3);% change in recovered
population

end

[t,x] = ode45(@sir, tperiod, [S0 I0 R0]);       % solves ODE

figure (1)
plot(t,x(:,1),'b',t,x(:,2),'r',t,x(:,3),'g','linewidth',1) %
plot solutions
xlabel('Time in Years'); ylabel('Population')           %
label axis
legend('S','I','R')                                % legend

beta = 0.00265;                % rate of infection
gamma = 26;                    % rate of recovery
mu = 1/2;                      % natural death rate
lambda = N*mu;                 % birth rate


R = (lambda*beta)/((gamma+mu)*mu)        % basic reproduction
number
```

```
eqm=[lambda/(mu*R) mu/beta*(R-1)]       % endemic equilibrium
values (S, I)


for I0 = [1,10000:10000:50000]  % initial infected populations
for
    ... phase portrait

    S0 = N-(I0+R0);             % initial susceptible
population

    [t,x] = ode23s(@sir, tperiod, [S0 I0 R0]); % solves ODE

    SF = x(:,1)./N;             % susceptible population
fraction
    IF = x(:,2)./N;             % infected population fraction
    T=1-SF;                     % triangle indicating S + I <
1

    figure (2)
    plot(SF,IF,'b',SF,T,'k','linewidth',.5); ylim([0 1]);   %
plot
    ... phase plane
    xlabel('Susceptible Population Fraction'); % label axis
    ylabel('Infected Population Fraction');
    hold on

end

for R0 = 10000:10000:30000      % initial removed populations
for phase plane

    I0 = 1;                     % initial infected population
    S0 = N-(I0+R0);             % initial susceptible
population

    [t,x] = ode45(@sir, tperiod, [S0 I0 R0]);   % solves ODE

    SF = x(:,1)./N;             % susceptible population
fraction
    IF = x(:,2)./N;             % infected population fraction

    plot(SF,IF,'b','linewidth',.5)  % plot phase plane
    hold on
end
legend('Trajectory','T')        % phase portait legend
plot(eqm(1)./N,eqm(2)./N,'rx','DisplayName','Fixed Point')  %
plot fixed
```

```
    ... point

end
```

Appendix 6 – SIR Data Fitting Model Code

```
function SIR_fit

load school_data.txt          % load data
format long                   % precision

day = school_data(:,1);       % time coordinates of data
cases = school_data(:,2);     % number of cases each day

tforward = 3:0.01:20;         % time period ODE solved over
tpoints = [1:100:1101]';      % selects the solution data points
    ... corresponding to real data points given for
comparision

gamma = 0.3;                  % initial recovery rate estimate
beta = 0.0025;                % initial infection rate estimate
k = [gamma beta];             % parameters
N = 763;                      % total population
I0 = 25;                      % initial infected population
R0 = 0;                       % initial recovered population
S0 = N-(I0+R0);               % initial susceptible population

function dx = SIR_school(t,x,k)     % SIR equations

gamma = k(1);                 % current estimate for recovery
rate
beta = k(2);                  % cureent estimate for infection
rate
dx = zeros(3,1);              % assigns zeros to dx

dx(1) = x(2) * x(1) * -beta;     % change in susceptible
population
dx(2) = x(2) * x(1) * beta - x(2) * gamma; % change in
infected population
dx(3) = gamma * x(2);            % change in removed population

end

[T X] = ode23s(@(t,x)(SIR_school(t,x,k)),tforward,[S0 I0 R0]);
                              % solves ODE for plot
Ie = X(:,2);                  % infected population estimate
```

```
figure(1)
subplot(2,2,1);
plot(day,cases,'r.');       % plot real data
hold on
plot(T,Ie,'b-');            % plot infected population
estimate
    ... using initial parameter values
ylabel('Number of Cases');  % label axis
xlabel('Time in Days');
legend('Real Data','SIR Model');
axis([3 20 0 500]);         % axis limits

function error = SSE(k)     % error sum of squares

[T X] = ode23s(@(t,x)(SIR_school(t,x,k)),tforward,[S0 I0 R0]);
                            % solves ODE for SSE

cases_estimate = X(tpoints(:),2); % infected population
estimate

error = sum((cases_estimate - cases).^2); % calculates error
sum of squares
    ... between estimated and real data
end

[k,min_error] = fminsearch(@SSE,k);  % adjust parameter values
to find
    ... minimum value for error and assign final paramaters to
k

gamma = k(1)                % display final recovery rate
beta = k(2)                 % display final infection rate
R = N*(k(2)/k(1))           % display reproduction number


[T X] = ode23s(@(t,x)(SIR_school(t,x,k)),tforward,[S0 I0
R0]); % solve ODE
    ... with new parameter values

If = X(:,2);                % final infected population
estimate

subplot(2,2,2)
plot(day,cases,'r.');       % plot real data
hold on
plot(T,If,'b-');            % plot estimated value of infected
population
    ... with final parameter values
```

```
ylabel('Number of Cases');  % label axis
xlabel('Time in Days');
legend('Real Data','SIR Model');    % legend
axis([3 20 0 500]);          % axis limits

subplot(2,2,3)
plot(T,X(:,1),'b-',T,X(:,2),'r',T,X(:,3),'y');   % plots of
    ... susceptible, infected and removed populations against
time
xlabel('Days'); ylabel('Number of People');     % label axis
legend('S','I','R');         % legend
axis([3 20 0 800]);          % axis limits

SF = X(:,1)./N;              % susceptible population fraction
IF = X(:,2)./N;              % infected population fraction

subplot(2,2,4)
plot(SF,IF,'r');             % plot phase plane
xlabel('Susceptible Population Fraction');  % label axis
ylabel('Infected Population Fraction');
axis([0 1 0 0.6]);           % axis limits

end
```

Appendix 7 – SIR Data Fitting Model .txt File

school_data.txt

3,25

4,75

5,227

6,296

7,258

8,236

9,192

10,126

11,71

12,28

13,11

14,7

Appendix 8 – Avian Influenza Parameter Fitting Model Code

```
function BirdFluModel2020

load BirdFluData2020.txt          % imports the bird flu data
tdata = BirdFluData2020(:,1);     % time in years
qdata = BirdFluData2020(:,2);     % number of cumulative cases

tforward = (0:0.01:15)';          % time span for ODE solutions
tmeasure = [1:50:1501]';          % selects points in the
solution for
    ... comparison with data

format long                       % precision

Hpop = 26370;                     % human population of
countries affected
    ... in units of 10^5
Bpop = 16540;                     % poultry population of
countries affected
    ... in units of 10^6
Ih0 = 0.0005;                     % initial infected human
population
    ... in units of 10^5
betaB = 0.002;                    % initial estimate for
transmission rate
    ... in poultry population
betaH = 1e-8;                     % initial estimate for
transmission rate
    ... between birds and humans
Ib0 = 5;                          % inital estimate for infected
    ... bird population

k = [betaB betaH Ib0];            % initial values of parameters
to be fitted


function dx = SISI(t,x,k)         % SISI equations

lambdaB = 8270;                  % poultry birth rate
lambda = 26370/65;               % human birth rate
muB = 1/2;                       % poultry natural death rate
nuB = 36.5;                      % poultry death rate due to AI
mu = 1/65;                       % human natural death rate
nu = 36.5;                       % human death rate due to AI
dx = zeros(5,1);                 % assigns zeros to dy
```

```
dx(1) = lambdaB-k(1)*x(2)*x(1)-muB*x(1);    % change in
susceptible
    ... bird population
dx(2) = k(1)*x(2)*x(1)-(nuB+muB)*x(2);      % change in
infected
    ... bird population
dx(3) = lambda-k(2)*x(2)*x(3)-mu*x(3);      % change in
susceptible
    ... human population
dx(4) = k(2)*x(3)*x(2)-(nu+mu)*x(4);        % change in
infected
    ... human population
dx(5) = k(2)*x(3)*x(2);                     % cumulative cases
(no deaths)

end

function cases = Inf_hum(k,tdata)     % solves ODEs to give
cumulative
    ... cases values to be compared with real data

[T X] = ode23s(@(t,x)(SISI(t,x,k)),tforward,[Bpop-k(3) k(3)
Hpop Ih0 Ih0]);
    % solves ODEs with initial conditions
 cases = X(tmeasure(:),5);       % case values corresponding to
real data

end

lb = [0 0 0];                    % sets lsqcurvefit lower bound

for i = 1:5

 [k,resnorm,residual] =
lsqcurvefit(@Inf_hum,k,tdata,qdata,lb,[],...
 optimset('TolX',10^(-20),'TolFun',10^(-20)));
    % uses SSE and assigns parameters that give the minimum
amount of error
    ... to k

end

[T X] = ode23s(@(t,x)(SISI(t,x,k)),tforward,[Bpop-k(3) k(3)
Hpop Ih0 Ih0]);
    % solve ODEs with new parameter values

lambdaB = 827;                   % poultry birth rate
muB = 1/2;                       % poultry natural death rate
```

```
nuB = 36.5;                         % poultry death rate due to AI

betaB = k(1)                        % display parameter values
betaH = k(2)
Ib0 = k(3)
Rb = (lambdaB*betaB)/(muB*(muB+nuB))    % display basic
reporduction number
    ... for bird population

cases_data = qdata.*10^5;               % change units from
10^5 to 1
cases_calc = X(:,5).*10^5;              % change units from
10^5 to 1
year = 2005+T;                          % change time to year
year_data = 2005+tdata;                 % change time to year

plot(year_data,cases_data,'r.');        % plot real data
hold on
plot(year,cases_calc,'b-');             % plot curve
xlabel('Year');                         % label axis
ylabel('Cumulative Number of Cases');
legend('real data','equation solution') % legend

end
```

Appendix 9 – Avian Influenza Parameter Fitting Model .txt File

0	0.00047
0.5	0.00108
1	0.00148
1.5	0.00229
2	0.00263
2.5	0.00318
3	0.00351
3.5	0.00387
4	0.00395
4.5	0.00436
5	0.00467
5.5	0.005
6	0.00516

6.5	0.00562
7	0.00576
7.5	0.00607
8	0.00610
8.5	0.00633
9	0.0065
9.5	0.00789
10	0.00793
10.5	0.00797
11	0.00803
11.5	0.00806
12	0.00807
12.5	0.00807
13	0.00807
13.5	0.00808
14	0.00808
14.5	0.00808
15	0.00809

Appendix 10 – Avian Influenza Results Plotting Model Code

```
function BirdFlu_results

format long                         % precision

tforward = (0:0.01:30)';            % time span for ODE solutions

Hpop = 26370;                       % human population of
countries affected
    ... in units of 10^5
Bpop = 16540;                       % poultry population of
countries affected
    ... in units of 10^6
Ih0 = 0.0005;                       % initial infected human
population
    ... in units of 10^5
```

```
betaB = 0.002243299639567;      % transmission rate in poultry
population
betaH = 0.000000015703248;      % transmission rate between
birds and humans
Ib0 = 2.55443354741183;         % infected bird population

k = [betaB betaH Ib0];          % fitted parameters


function dx = SISI(t,x,k)       % SISI equations

lambdaB = 8270;                 % poultry birth rate
lambda = 26370/65;              % human birth rate
muB = 1/2;                      % poultry natural death rate
nuB = 36.5;                     % poultry death rate due to AI
mu = 1/65;                      % human natural death rate
nu = 36.5;                      % human death rate due to AI
dx = zeros(7,1);                % assigns zeros to dy

dx(1) = lambdaB-k(1)*x(2)*x(1)-muB*x(1);    % change in
susceptible
    ... bird population
dx(2) = k(1)*x(2)*x(1)-(nuB+muB)*x(2);      % change in
infected
    ... bird population
dx(3) = lambda-k(2)*x(2)*x(3)-mu*x(3);      % change in
susceptible
    ... human population
dx(4) = k(2)*x(3)*x(2)-(nu+mu)*x(4);        % change in
infected
    ... human population
dx(5) = k(2)*x(3)*x(2);                     % cumulative cases
(no deaths)
dx(6) = nuB*x(2);                           % total poultry
deaths due to AI
dx(7) = (nuB+muB)*x(2) - muB*x(7);
end

[T X] = ode23s(@(t,x)(SISI(t,x,k)),tforward,[Bpop-k(3) k(3)
Hpop Ih0 Ih0 0 0]);
    % solve ODEs

lambdaB = 8270;                 % poultry birth rate
lambda = 26370/65;              % human birth rate
muB = 1/2;                      % poultry natural death rate
nuB = 36.5;                     % poultry death rate due to AI
```

```
Rb = (lambdaB*k(1))/(muB*(muB+nuB))     % display basic
reporduction number
    ... for bird population


cases_calc = X(:,5).*10^5;              % change units from
10^5 to 1
year = 2005+T;                          % change time to year

figure (1)                              % human cases curve
plot(year,cases_calc,'b-');             % plot curve
xlabel('Year');                         % label axis
ylabel('Cumulative Number of Cases');

figure (2)                              % total poultry deaths
due to AI
poultry_deaths = X(:,6).*10^6;          % Change units from
10^6 to 1
plot(year,poultry_deaths,'r');          % plot curve
xlabel('Year');                         % label axis
ylabel('Total Number of Poultry Deaths due to AI');

figure (3)                              % phase plane plot
plot(X(:,1)*10^6,X(:,2)*10^6,'b');      % change units and
plot phase plane
xlabel('Susceptible Bird Population');  % label axis
ylabel('Infective Bird Population');
hold on
eqm = [lambdaB/(muB*Rb) (muB/betaB)*(Rb-1)] % calculate fixed
point
plot(eqm(1)*10^6,eqm(2)*10^6,'kx');         % plot fixed point
legend('Trajectory', 'Endemic Equilibrium') % legend

figure (4)                              % infected population
against time
plot(year,X(:,2)*10^6,'r')              % plot curve
xlabel('Year')                          % label axis
ylabel('Infected Bird Population')
ylim([0 3e6])                           % y axis limit

figure (5)                              % susceptible
population against time
plot(year,X(:,1)*10^6,'b')              % plot curve
xlabel('Year')                          % label axis
ylabel('Susceptible Bird Population')

figure (6)                              % removed population
against time
```

```
plot(year,X(:,7)*10^6,'g')                % plot curve
xlabel('Year')                            % label axis
ylabel('Removed Bird Population')

S_eqm=lambda/(k(2)*eqm(2)+1/65);              % susceptible
human equilibrium
I_eqm=(k(2)*S_eqm*eqm(2))/(1/65+36.5);        % infected human
equilibrium
rho=1/74;                                     % dimensionless
quantity
discriminant=(rho*Rb)^2-4*(rho*Rb-rho);       % eigenvalue
discriminant
R_eqm=(nuB/betaB)*(Rb-1);                     % removed bird
equilibrium
dI=betaH*S_eqm*eqm(2);                        % human infections
per year at equilibrium
dR=nuB*eqm(2);                                % bird deaths per
year at equilibrium

figure (7)                % nullcline plot
R=Rb;                     % basic reproduction number
x1=[0:0.1:1.2];           % horizontal y-nullcline x values
y1=zeros(1,13);           % horizontal y-nullcline y values
x2=1/R.*ones(1,15);       % vertical y-nullcline x values
y2=[-0.2:0.1:1.2];        % vertical y-nullcline y values
plot(x1,y1,'b--');        % plot horizontal y-nullcline
hold on
plot(x2,y2,'b--');        % plot vertical y-nullcline
hold on
legend('y-nullcline')     % legend

x3=[0.01:0.01:1.2];           % x-nullcline x values
y3=(rho/R).*(1-x3)./x3;       % x-nullcline y values
plot(x3,y3,'r--','DisplayName','x-nullcline')   % x-nullcline
ylim([-.5e-4 1e-4])           % axis limits
xlim([0.994 1.002])
hold on

eqm1=[1,0];                   % disease free equilibrium
plot(eqm1(1),eqm1(2),'kx','DisplayName','Disease-Free
Equilibrium')
% plot disease free equilibrium
eqm2=[1/R,rho*(1-1/R)];
% endemic equilibrium
plot(eqm2(1),eqm2(2),'ko','DisplayName','Endemic Equilibrium')
% plot endemic equilibrium
plot(X(:,1)/Bpop,X(:,2)/Bpop,'b','DisplayName','Trajectory');
```

```
% plot dimensionless susceptible population against infective
ylim([-0.5e-4 3e-4])     % axis limits
xlim([0.99 1.004])
xlabel('xb')             % label axis
ylabel('yb')
end
```

Appendix 11 – Avian Influenza Model Initial Parameter Estimates

Initial β_b	0.002	0.002	0.002	0.002	0.002	0.002
Initial β	0.00000005	0.00000005	0.00000005	0.00000005	0.00000005	0.00000005
Initial I_{b0}	3	3.5	4	4.5	5	5.5
Fitted β_b	0.00225671	0.002241747	0.00224172	0.002254127	0.002252107	0.002244137
Fitted β	8.59775E-09	1.80339E-08	1.8142E-08	9.44601E-09	1.02447E-08	1.53792E-08
Fitted I_{b0}	4.048987215	2.223844881	2.20474587	3.776917349	3.54642266	2.543096961
$\mathcal{R}_b$	1.008810185	1.002121465	1.00211094	1.007655733	1.006752527	1.003189894
Error	2.53467E-07	2.43541E-07	2.3817E-07	2.48342E-07	2.44779E-07	2.35042E-07

Initial β_b	0.002	0.002	0.002	0.002	0.002	0.002
Initial β	0.00000005	0.0000001	0.00000015	0.0000002	0.00000025	0.0000003
Initial I_{b0}	5.5	5.5	5.5	5.5	5.5	5.5
Fitted β_b	0.002244137	0.002240682	0.00223583	0.002234213	0.002236187	0.002233446
Fitted β	1.53792E-08	1.96473E-08	3.2584E-08	4.17398E-08	3.10582E-08	4.81839E-08
Fitted I_{b0}	2.543096961	2.056891614	1.29351251	1.02441052	1.353256091	0.893332856
$\mathcal{R}_b$	1.003189894	1.001645473	0.99947733	0.998753455	0.999636226	0.998410716
Error	2.35042E-07	2.35728E-07	2.3679E-07	2.36766E-07	2.35874E-07	2.38566E-07

Initial β_b	0.001	0.002	0.003	0.004	0.005
Initial β	0.00000005	0.00000005	0.00000005	0.00000005	0.00000005
Initial I_{b0}	5.5	5.5	5.5	5.5	5.5
Fitted β_b	0.002252272	0.002244137	0.00225149	0.002242075	0.00224382
Fitted β	1.01673E-08	1.53792E-08	1.0505E-08	1.76568E-08	1.56325E-08
Fitted I_{b0}	3.57152738	2.543096961	3.48315858	2.259823911	2.51721665
$\mathcal{R}_b$	1.006826604	1.003189894	1.00647681	1.002268269	1.003048268
Error	2.45163E-07	2.35042E-07	2.4401E-07	2.35414E-07	2.35111E-07

Appendix 12 – Avian Influenza Model Equilibria Stability Analysis Working

Equilibriums are found by setting equations 77 and 78 to 0.

$$x_b' = \rho_b(1 - x_b) - \mathcal{R}_b x_b y_b = 0,$$

$$y_b' = (\mathcal{R}_b x_b - 1)y_b = 0,$$

There are two equilibriums, the disease free equilibrium where $y_b = 0$ and $x_b = 1$, and the endemic equilibrium, where $x_b = 1/\mathcal{R}_b$ and $y_b = \rho_b(1 - 1/\mathcal{R}_b)$. The endemic equilibrium only exists if $\mathcal{R}_b > 1$ as the boundary of the feasible region is $x_b \geq 0, y_b \geq 0$.

Dimensionless disease free equilibrium

$$\mathcal{E}_0 = (1,0),$$

Dimensionless endemic equilibrium

$$\mathcal{E} = \left(\frac{1}{\mathcal{R}_b}, \rho_b\left(1 - \frac{1}{\mathcal{R}_b}\right)\right),$$

The stability of the equilibria can be found by using the Jacobian matrix:

$$J(x_b, y_b) = \begin{bmatrix} -\rho_b - \mathcal{R}_b y_b & -\mathcal{R}_b x_b \\ \mathcal{R}_b y_b & \mathcal{R}_b x_b - 1 \end{bmatrix},$$

The Jacobian matrix for the disease free equilibrium is:

$$J(1,0) = \begin{bmatrix} -\rho_b & -\mathcal{R}_b \\ 0 & \mathcal{R}_b - 1 \end{bmatrix},$$

Giving eigenvalues of:

$$\lambda_1 = -\rho_b, \qquad (80) \quad \lambda_2 = \mathcal{R}_b - 1, \qquad (81)$$

The Jacobian matrix for the endemic equilibrium is:

$$J\left(\frac{1}{\mathcal{R}_b}, \rho_b\left(1 - \frac{1}{\mathcal{R}_b}\right)\right) = \begin{bmatrix} -\mathcal{R}_b\rho_b & -1 \\ \mathcal{R}_b\rho_b - \rho_b & 0 \end{bmatrix},$$

Giving eigenvalues of:

$$\lambda_{1,2} = \frac{-\rho_b\mathcal{R}_b \pm \sqrt{(\rho_b\mathcal{R}_b)^2 - 4(\rho_b\mathcal{R}_b - \rho_b)}}{2}, \qquad (82)$$